Pool fire burning characteristics and risks under wind-free conditions

State-of-the-art

Guo, Youwei; Xiao, Guoqing; Wang, Lingyuan; Chen, Chao; Deng, Hongbo; Mi, Hongfu; Tu, Chu; Li, Yuanyuan

DOI
10.1016/j.firesaf.2023.103755

Publication date
2023

Document Version
Final published version

Published in
Fire Safety Journal

Citation (APA)
Guo, Y., Xiao, G., Wang, L., Chen, C., Deng, H., Mi, H., Tu, C., & Li, Y. (2023). Pool fire burning characteristics and risks under wind-free conditions: State-of-the-art. *Fire Safety Journal*, *136*, Article 103755. https://doi.org/10.1016/j.firesaf.2023.103755

Fire Safety Journal 136 (2023) 103755

Contents lists available at ScienceDirect

Fire Safety Journal

journal homepage: www.elsevier.com/locate/firesaf

Pool fire burning characteristics and risks under wind-free conditions: State-of-the-art

Youwei Guo [a], Guoqing Xiao [a,b,g,*], Lingyuan Wang [a], Chao Chen [e,f], Hongbo Deng [a], Hongfu Mi [c], Chu Tu [d], Yuanyuan Li [a]

[a] College of Chemistry and Chemical Engineering, Southwest Petroleum University, Chengdu, Sichuan, 610500, China
[b] Oil & Gas Fire Protection Key Laboratory of Sichuan Province, Chengdu, Sichuan, 611731, China
[c] College of Safety Engineering, Chongqing University of Science&technology, No. 20 Daxuecheng East Road, Chongqing, 401331, China
[d] Institute of Computing Technology, Chinese Academy, 6 Zhongguancun South Road, Haidian District, Beijing, 100086, China
[e] Safety and Security Science Group, Faculty of Technology, Policy and Management, TU Delft, Delft, the Netherlands
[f] School of Petroleum Engineering, Southwest Petroleum University, Chengdu, Sichuan, 610500, China
[g] Gas Reservoir Geol & Exploita, Chengdu, 610500, Sichuan, China

ARTICLE INFO

Keywords:
Pool ire
Mass burning rate
Fire risk
Flame height
Radiation

ABSTRACT

Pool fire is a typical example of fire accidents in chemical process industries. Since fire researchers have implemented a variety of measurements to gain insights into pool fire and to prevent fire disasters, there is a need to illustrate how pool fire models influence the risk assessment results. This review intends to consecutively discuss the effect of different physical factors on the burning behavior of pool fire and fire risk assessment. For the most part, this review extracts representative works from abundant pool fire articles in the last years and is subdivided into mass burning rates, entrainment, flame height, pulsation, radiation transfer sections, and risk assessment. On the basis of the latest research, it is indicated that new fire models can provide more accurate and reliable assessment results than previous models. They are not only to reduce the cumbersome work and resources but also to validate computational fluid dynamics (CFD) models that are essential components of performance-based design in fire prevention. Consequently, providing the latest information about how pool fire evolves and how risk assessment is affected, this review paper would be advantageous to fire experts in the future.

1. Introduction

On December 11, 2005, after explosions a major fire occurred at an oil storage facility in Buncefield, causing 43 people to be injured and economic losses of nine hundred million pounds. In the scenes of fire, flammable liquid pools formed after liquid fuels were released on the ground and reached fire embankments. When the pools were ignited, a turbulent diffusion fire burning appeared above the horizontal pool surface of vaporizing hydrocarbon fuels, a fire situation that is called "pool fire". Of all the uncontrolled fire scenarios, statistically, pool fire accounts for nearly 42% of whole fire accidents [1]. Many fire researchers have investigated the burning characteristics of the pool fire and managed to reduce the probability of such fire disasters.

Pool fire is a typical diffusion flame, which is thought to have low-initial momentum on the horizontal burning surface above which most of the reaction rates are higher than mixing rates [2]. The diffusion flames are forced-flow, buoyancy-flow, or mixed-flow without some characteristics, such as flame velocity. These flows, during the burning process, would be enhanced because exothermic chemical reactions cause significant temperature differences and thus a greater density gradient [3]. Fig. 1 shows the main morphological characters of a pool fire.

In the previous investigation into pool fire, the most important parameters are identified [4–7]: mass burning rate and heat release rate (HRR). Studies have shown that both parameters will vary obviously with the change in initial fuel temperatures, pressure, oxygen concentrations, etc. And many causal studies concerning the environmental and fuel types effect have also been carried out under the bench scale without cross flow because fire researchers are to handle experiments and data more easily than they would otherwise. Specifically, Pressure change would affect the soot yields and flame length [8,9]; temperature

* Corresponding author. Southwest Petroleum University, Chengdu City, Sichuan Province, 610500, China.
E-mail address: xiao13541694312@163.com (G. Xiao).

https://doi.org/10.1016/j.firesaf.2023.103755
Received 28 February 2022; Received in revised form 24 October 2022; Accepted 29 January 2023
Available online 7 February 2023

Nomenclature

A	pool surface area (m^2)
St	Strouhal number $St = fD/V$
D	pool diameter (m)
T_f	flame temperatures (K)
D_{eff}	the modified perimeter-equivalent diameter, $D_{eff} = 2(L+W)]/\pi$ (m)
T_s	the pool surface temperature (K)
D^*_{eff}	D^*_{eff} is the perimeter-equivalent diameter based on 'mirror' approach considering the effect of air entrainment (m)
T_∞	the ambient temperature (K)
d	lip height (m)
$\dot{y}_c$	thermal penetration rate (m/s)
c_p	the heat capacity of air taken at average combustion temperature ($J/(kg \cdot K)$)
x_i	the number of deaths for corresponding accidents
E_f	the total emissive power of the flame at the fire surface (kW)

Greek

F_r	Froude number, the ratio of inertial forces to the buoyant forces $F_r = u^2/gl$
χ_a	actual heat fraction of ideal heat release rate
F	view factor
χ_R	the radiation fraction of the heat release
f_i	the frequency of an accident type i (events/year)
ρ_∞	ambient air density
G_r	Grashof number, the ratio of the buoyancy to the viscous force acting on a fluid $G_r = (\Delta\rho/\rho)(gl^3/\nu^2)$
σ	Stefan-Boltzmann constant ($5.670373 \cdot 10^{-8} W \cdot m^{-2} \cdot K^{-4}$)
g	the force of gravity (m/s^2)
φ_{br}	the liquid burning rate to its base value with no lip
H_c	lower heating value per unit mass (kJ/mol)
θ	an angle between the normal to the target and the line from source to the target
ΔH_g	heat of gasification (kJ/mol)
ε_f	the emissivity of a flame
h	the convective heat transfer coefficient ($W/m^2 \cdot K$)
τ	atmospheric transmissivity
K_s	soot absorption coefficient (m^{-1})

Subscripts

L	average flame height (m)
f	flame
L_C	length of the bottom of pool fire "clean burning zone" (m)
∞	ambient
L_I	length of the intermittency zone (m)
s	flame surface
L_m	beam length (m)
$\dot{m}''$	mass burning rate per unit area ($g/m^2 \cdot s$)
$\dot{m}_{ent}$	air entrainment rate (g/s)
N	a dimensionless parameter for fitting flame height
N^*	a dimensionless parameter for fitting flame height under different ambient oxygen concentrations
$\dot{Q}$	heat release rate (kW/s)
$\dot{Q}_r$	the total radiative energy output of the fire (kW/s)
Q^*_D	a dimensionless parameter for fitting flame height
$\dot{q}''_f$	heat flux transfer from the flame to the pool ($kW/m^2 \cdot s$)
$\dot{q}''_{f,rad}$	the radiation heat transfer per unit area per second from pool fires ($kW/m^2 \cdot s$)
r	the stoichiometric mass ratio of fuel to air
r_{ir}	the individual risk of death
Ri	a ratio of buoyancy forces to inertia forces $Ri = [(\rho_\infty - \rho_p) gD]/\rho_\infty V^2$
R	the distance from the point source to the target

change in the bottom of the burner would lower or increase the mass burning rate [10–13]; radiation disturbance would strongly interfere with the heat balance [14–16]. With the combination of these factors, the degree of pool fire can be classified through a range of Froude numbers (the ratio of inertial forces to the buoyant forces): intermediate scale pool fires, large pool fires, and mass fires. These results indicate that the pool fire can be strongly affected by dimensional factors (e.g. pool diameters) and environmental conditions, thus precluding fire researchers from accurately assessing fire risks in chemical industries [17].

In fire scenes, pool fire would damage adjacent equipment, trigging domino events. The domino effect will accelerate fire propagation and consequently causes serious aftermath in the chemical process industries. Many researchers have discussed the domino risk assessment and the way to model and manage domino effects in the process industries [18,19]. However, since many articles separately discuss the burning characteristics of pool fire and the risk assessment of fire scenarios, the relationship between the burning behavior of pool fire and their risk assessment has less been discussed.

To the best of our knowledge, the radiation output, for example, is a

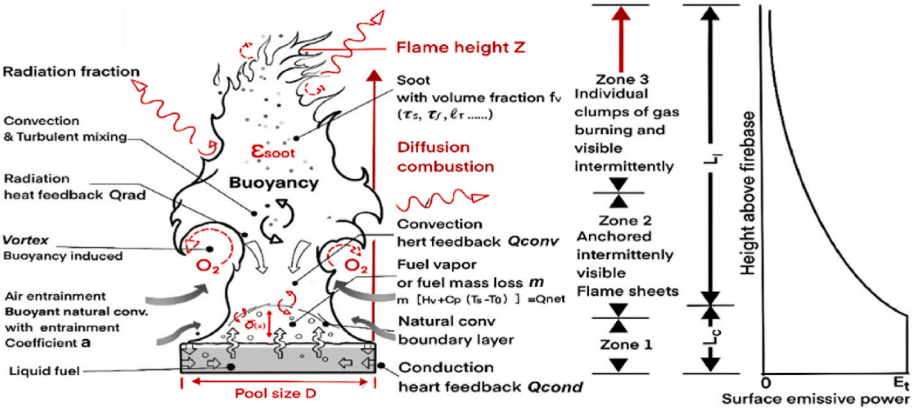

Fig. 1. The schematic depiction of pool fires under wind-free conditions [20].

significant escalation vector in fire risk assessment (Table 1). This radiative energy incident to external targets could be easily influenced by the change in the burning conditions of pool fire. As can be seen from Table 2, this change is linked with many parameters, ranging from heat balance mechanism to combustion products.

Based on previous research, in this study we aim to develop an understanding of how these parameters would disturb the fire risk assessment when pool dimensions and environmental conditions vary. The latest fire models and data are included in this review. These models are more useful for describing pool fire evolvement and calculating fire safety distances in chemical process industries.

The outline of this study is as follows. Section 3 displays the main characteristics of the pool fire burning: 1. The effect of pool scales, pressure, boilover, and air entrainment on the mass burning rate. 2. The calculation and application of flame height in the process industries. 3. Pulsation behavior and the radiation heat transfer. Section 4 presents a risk assessment referring to the fire scenario. Section 5 discusses the potential relationships between those parameters and the limitations of some approaches. Section 6 concludes implications from the discussion and recommendations for future work.

2. Method

Based on the systematic review technique [22], four steps were taken to review the current pool fire research issues and methods in the chemical and process industries. Firstly, we proposed the research questions in light of the notions mentioned in Section 1.

1. What are the important parameters on which fire engineers focus?
2. What are the accepted fire models for dealing with calculations such as radiation?
3. What are the relationships between pool fire burning and its risk assessment?
4. What are the implications and limitations of established inferences?

Over 400 articles were searched from the online resource: (i) Web of Science, (ii) ScienceDirect. Keywords defined to facilitate the searching process includes “burning rate”, “boilover”, “pressure”, “air entrainment”, “flame height”, “pulsation”, “radiation”, “heat balance”, “risk assessment”, “domino”, “societal risk”, “liquid fuels”. Of all the articles extracted from the databases, we meticulously chose 184 articles according to the relevance of our objectives. These papers were gathered from Journal of Hazardous Materials, Fire Safety Journal, Combustion and Flame, Fuel, Proceeding of the Combustion Institute, Safety Science, NIST report, Combustion Science and Technology, and Journal of Loss Prevention in the Process Industries. The search result indicates that publications concerning pool fire have gradually increased over the last decade. Finally, we allocate, summarize, organize, and contrast the conclusions attained from the picked articles.

3. An overview of influential physical factors of pool fire

The investigation on pool fire covers burning kinetics, fluid dynamics, heat transfer, and other aspects related to the combustion process. From these theories it is shown that the evolvement of pool fire varies when physical and dimensional factors change [23–25]. As a result, we will consider the impact of influential factors in the following discussions.

Table 1
Physical effects responsible for the escalation of fire domino accidents in chemical industries [18].

Primary scenario	Escalation vector	Expected secondary scenarios
Pool fire	Radiation, fire impingement	Jet fire, pool fire, BLEVE, toxic release
Jet fire	Radiation, fire impingement	Jet fire, pool fire, BLEVE, toxic release
Fireball	Radiation, fire impingement	Tank fire
Fire impingement	Tank fire	

Table 2
Important parameters for the characteristics of pool fires [21].

	Transport mechanism	Relevant characteristic time	Regime of interest	Key issues
Fuel	diffusion	transport time	adjacent to the fuel surface	energy balance
	natural convection	reaction time	within the flame	soot production
Oxidizer	natural convection	entrainment time	close to the edge of the fuel	air entrainment
		plume residence time	far-field from the flame	residual oxygen concentration
Products	natural convection	species residence time	above the fuel surface	Toxicity heat transfer soot production and consumption
Energy	diffusion	Radiation feedback	everywhere	Controlling mechanisms
	conduction	radiation losses		Radiative feedback
	convection entrainment convection and far-field times	conduction		Far-field parameter profiles

3.1. Mass burning rate

Many early investigations into pool fire were set up on relatively small diameters. Nevertheless, when finding that the mass burning rate does not increase linearly with growing pool diameters, fire researchers realized that the scale effect is so important that it is necessary to carry out more studies on medium and large pool fires. In 1957, Blinov et al. [26] conducted experimental studies covering a wide range of pool diameters to show the relationship between pool diameters and mass burning rate (Fig. 2). The results prove that from 0.1 m to 0.5 m pool diameters the radiative heat transfer is dominant against convective transfer. And it is interesting to point out that for all types of fuels, the curve of the mass burning rate has the same trend. First, the mass burning rate decreases with increasing pool diameters, a laminar flow regime with Reynolds number around 20. With further growth of pool

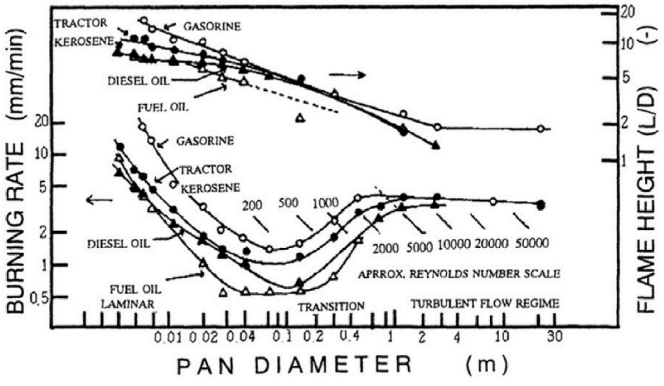

Fig. 2. Liquid burning rate and flame height as the function of fire regime in pool fires in still air [26].

diameters, the mass burning rate begins to increase in view of the Reynolds numbers from 20 to 200, and the slope starts to level off when the regime is turbulent with the Reynolds number above 500. Finally, the mass burning rate is reached nearly constant unaffected by the diameter and the fuel type when the pool diameter is about over 1 m, a level that may be caused by the formation of a fuel vapor core region attenuating heat feedback intensity. Fig. 2 also shows how flame height varies with pool diameters. The dimensionless flame height (flame height divided by the pool diameter) declines rapidly if pool diameters increase and then the trend seems to be stable for larger pools with a factor of 2.

In 1959, Hottel [27] reviewed the work of Blinov and Khudiakov and proposed a meaningful analysis of correlations between the heat flux $\dot{q}_f''$ transferred from the flame to the pool and mass burning rate $\dot{m}''$. The equation can be written as:

$$\dot{q}_f'' = \frac{4\sum \dot{q}}{\pi D^2} = 4\frac{k_1(T_f - T_s)}{D} + k_2(T_f - T_s) + k_3\left(T_f^4 - T_s^4\right)[1 - \exp(-k_4 D)] \quad (1)$$

The form of energy transport can be divided into conduction, convection, and radiation. $\dot{q}_f''$ is the heat release rate per unit area, k_1 is the conductivity of materials incorporating extra heat transfer terms and k_2 is the convection coefficient, k_3 includes the Stefan-Boltzmann constant σ and the view factors, while the last term $1 - \exp(-k_4 D)$ is the effective emissivity of the flame in which k_4 is a correction factor or called extinction coefficient.

Mass burning rate is closely linked with radiation heat feedback from flames. Yumoto [28] measured radiation heat feedback by Gardon gauges at the medium-sized pool center using gasoline and hexane (0.6 m$< D <$3 m). The results concluded that the intensity of radiation at the pool edge was as half as that at the pool center, and it accounted for almost 65% of the heat feedback energy near the pool surface. Hamins [29] provided more details on the application of radiative measurements, pointing out that the burning rates were highest in the center of the burner, decreasing gradually away from the center and then increasing again at the edge of the burner [6]. Shinotake [30] found that under the larger pool diameters, the flame would be much closer to the pool surface in the initial transient stage than in the steady burning stage. From then on, the radiation flux in the initial burning stage is much larger, inducing the excess evaporation of liquid fuels. However, the volume of unburned fuel vapor may strongly block the radiation from the flame to the pool surface.

Tian [31]theoretically analyzed influencing factors of burning rate on the subject of the size of pools, initial temperature, and fuel thickness. In his work, lip height, defined as a distance from the pool surface towards the rim of a container, significantly impacts heat transfer efficiency and mass burning rate because it disturbs the flow structures near the pool surface and alters the dominant heat feedback mechanism. Babrauskas [32] quoted the Orloff's work on fires of PMMA, which refers to how the ratio of lip height to pool diameters, d/D, affected the ratio of the liquid mass burning rate to its value measured without lip height, as can be seen in Table 3.

Oxygen concentration is changeable in many places, such as in chemical and industrial processes, a vent-limited compartment, and high-altitude facilities, influencing the burning behavior of pool fire. In this study, the oxygen concentration is confined to ambient conditions since much research is carried out under different altitudes or pressure chambers aiming to stimulate atmospheric conditions. In order to investigate the evolvement of the burning process under different oxygen concentrations, Nasr et al. [33,34] implemented experiments with a pressure chamber and found that the mass burning rate, temperature variation, and heat feedback are very sensitive to the change of oxygen concentrations at the flame base. Results indicated that the flame radiation fraction decreases with the decline in oxygen concentration, whereas the convection fraction gradually increases. In 2019, Chen [35] investigated the oxygen concentration effect. Fig. 3 shows that the onset of the boiling burning stage would happen earlier under high oxygen concentrations, in contrast to the disappearance of the boiling when the oxygen concentration decreased to 15%. In addition, with a higher oxygen concentration the volume of soot would rise in the sense that the soot formation rate increases for high-temperature flames.

Table 3
Effect of the ratio d/D of the lip height to the pool diameter on the ratio φ_{br} of the liquid burning rate to it base value with no lip [32].

d/D	φ_{br}
0	1.0
0.07	1.6
0.2	2.0
>0.2	Slow decrease

3.2. Pressure & boilover effect

Altitude variance will result in different pressure conditions and hence changes the atmospheric oxygen concentration and mass burning rate. The effect of pressure has been discovered for the last decades to establish relationships between the burning behavior and pressure. The University of Science and Technology of China, for the most part, has carried out a series of experiments in Hefei and Tibet. According to the classic heat feedback theory by Drysdale [36] and scaling laws [37–39], when the diameter is greater than 20 cm, the radiation transfer is dominant in heat feedback, and the flame radiant heat fluxes $\dot{q}_{f,rad}''$ is

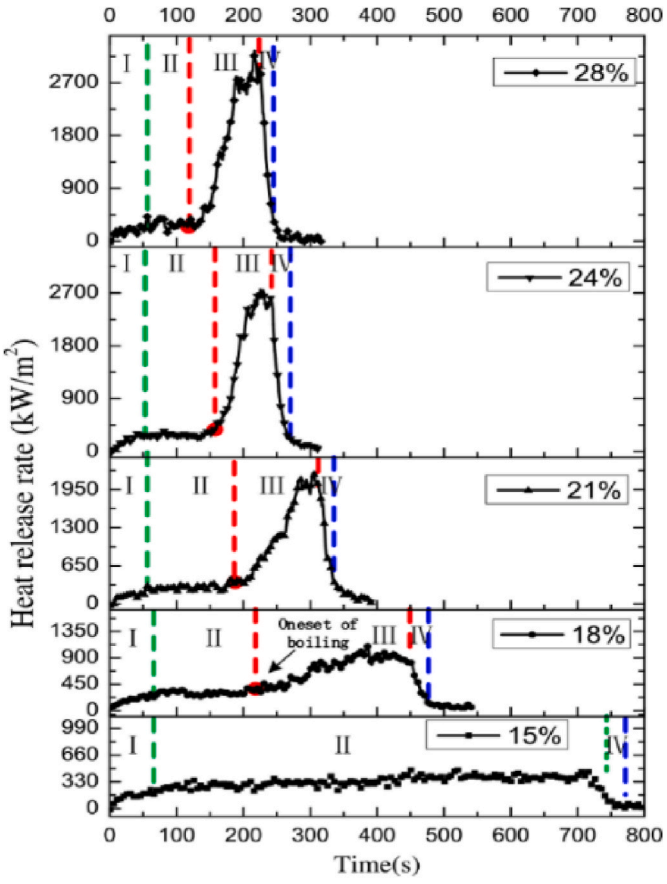

Fig. 3. Heat release rates for n-heptane pool fires under different oxygen concentrations (I initial growth stage, II steady burning stage, III boiling burning stage, IV decay stage) [35].

equal to:

$$\dot{q}''_{f,rad} = \sigma T_f^4 [1 - \exp(-K_s L_m)] \quad (2)$$

T_f is flame temperature, L_m is the beam length, and K_s is the soot absorption coefficient. On the basis of this equation and De Ris' work [37], Tu [40,41] has thoroughly discussed how pool fire evolves under lower pressure when the heat transfer mechanism is radiation-controlled. His results suggested that the mass burning rate decreased in conjunction with a decrease in emissivity, in that less soot yielded in the combustion process. This process also caused a rise in flame temperatures, leading to higher puffing frequencies based on Categen's theory [42]. Similar to this synergetic effect, which includes the influences of pressure and scales, Tang [43] investigated the aspect ratio of pool and fuel type effects under high latitude. He proposed that flame height would be slightly higher than that under normal pressure, and radiative intensity would increase with an upsurge in aspect ratio if the fuel is sooty. Moreover, the results proved that the flame radiation fraction is a weak function of pressure, which can be written as: $\chi_R \sim p^{0.45}\sigma T_F^4$. As can be seen in Fig. 4, even though the pool aspect ratio ranged from 1 to 8, the flame radiation fraction was almost the same. This may result from the coupling effect of flame temperature and weaker air entrainment under lower pressure.

Another aspect that researchers would concern is how flame pulsation is affected by lower pressure. Chen [44]analyzed flame images with a MATLAB program, and subdivided the pulsation model into 'tip--flickering' and 'nontip-flickering', two different pulsation behavior brought about by the fact that under lower pressure, the flame is laminar and air entrainment is weak supported by buoyancy. However, with the increase in pressure, large eddy and vortical structures appear so that air entrainment and the concentration gradient increase, leading to different behavior.

Boilover is one of the most hazardous cases for fire safety [45]. Pool fire may also be triggered when the flammable liquid spills onto water, especially for LNG. The occurrence of boilover will not only damage the equipment in fire scenarios but could also cause domino accidents meanwhile. One hundred forty-six firefighters and citizens were killed by a boilover accident in Tacoa Venezuela [46]. Enormous effort was devoted to studying the main factors affecting the boilover [42,43], such as initial thickness, pool diameter, and boiling point.

It should be noted that pure liquids burn with a surface temperature close to their boiling point; however, for liquid mixtures containing volatiles and water, the surface temperature is unfixed and gradually increases with time since the remaining liquid is less volatile. The burning of liquid mixtures forms a high-temperature isotherm layer called "hot zone", in which the temperature is greater than 120 °C. When the hot zone reaches the interface between fuel and water sublayer, a furious evaporation process of water can occur, generating massive vapor bubbles that convey the combustible liquid to the fuel surface if the vapor pressure suppresses the head of liquid. This process ejects hot oil from the fuel container and is known as "boilover".

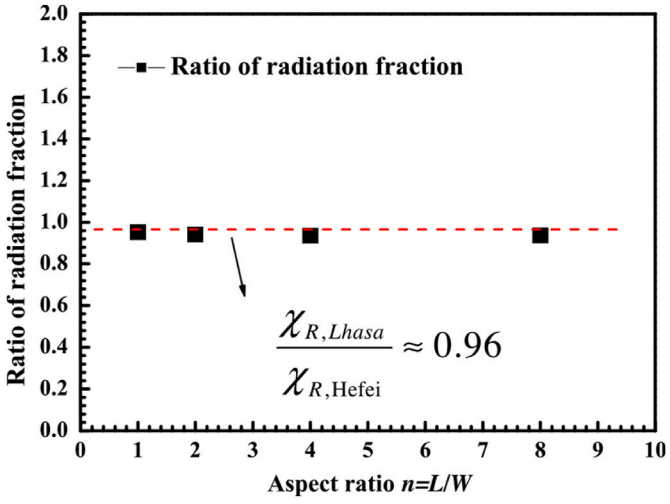

Fig. 4. Comparison of flame radiation fraction of rectangular thermal buoyancy source with aspect ratios in a normal and sub-atmospheric pressure [43].

In 1989, Hasegawa [47] discovered the mechanism of hot zone formation and found that vapor bubbles were scattered nearly homogenously in a hot zone, a conclusion similar to that of Hall [48], who was the first to investigate the hot zone, and Aria [49]. The evolvement of bubbles would cause energetic convection flow, including three processes: generation, ascent, and growth. The intensity of boilover is related to pool diameters and initial thicknesses of fuel [50], which decrease with the increasing pool diameters. It was observed that for same fuels the boilover was more intense with a higher fuel temperature, suggesting the hot zone temperature also depends on fuel types and the burning time. A series of experiments have been carried out using different moisture-content fuels, indicating that the burning process of fuel mixed with water is extremely different from that of pure fuels when combustion reaches a steady burning stage. And the formation of the hot zone is independent of the presence of water, whereas the water is indispensable for the occurrence of boilover.

When boilover occurs, it generally accompanies a noise referring to a crackling sound, and the fuel-water interface temperate is tested around $120^0C - 150^0C$, corresponding to the heterogeneous nucleation temperature of the water within pools [51,52]. In 1995, Fan [53]employed the spectrum analyzer to study the boilover premonitory period by recording a series of micro-explosion noises. The result demonstrated that this technique could be used to detect the onset of boilover from remote distances. Meanwhile, according to previous research, Ferrero [54] provided a way to calculate the thermal penetration rate:

$$\dot{y}_c = 0.056(1 - \exp(-2.2D)) \quad (3)$$

D is the diameter of burners. This equation can assess how fast the heat is transferred to the water interface. In recent years Kong et al. [55,56] investigated the burning characteristics of boilover with respect to flame enlargement and fuel temperature. It is found that four stages can be identified: the growth stage, quasi-steady stage, boilover stage, and decay stage. During the burning process, the boilover onset time was delayed with an increase in the initial fuel thickness but in inverse proportion to pool diameter, a result that corresponds to previous experiments. In addition, the boilover intensities increased with the initial fuel thickness and decreased with the pool diameter, suggesting that bubbles mixed with fuels enhance the mass burning rate in combustion.

Caution should be made that the onset time of boilover is linearly dependent on the initial layer thickness, while the impact of diameters is less important as opposed to small-scale experiments [57].

3.3. Air entrainment

After ignition, the ascent of the buoyant gases in the fire plume carries fire products to the outside, causing air to be entrained from the surroundings. Not only does this process supply air for the combustion of fuels, but it also dilutes and cools the fire products, which undergo a vertical movement. And there is a sharp increase in the quantity of soot generated by the fire.

In 1988, Koseki et al. [58] found that the total amount of air entrained is about five times that of the stoichiometric air needed to support combustion. In his result, sharp isothermal density plots suggested that air was entrained fiercely from the flame base near the edge of the pool to the core of the flame. Cetegen [59]delineated that the air entrainment process is the periodic engulfment of ambient air that surrounds the toroidal vortex rings and explained the frequency of vortex formation and crossing of those vortex rings in the combustion reaction zone. He previously suggested that plume mass flux is not a

function of the total fire heat release rate but a function of the source diameter and height in the visible flame region [60]. Meanwhile, the air entrainment process can be affected by pool geometry and environmental conditions such as a wall and corner. Tao [61,62] studied the sidewall effect on the air entrainment process and found that the air entrainment rate decreased when the fire source was gradually close to the sidewall, thus causing much higher flame height. And Tu [41] studied the effect of an aspect ratio of pool fire on the air entrainment process. He proposed that the air entrainment velocity is much larger on the short side of pool fire than on the long side, a result similar to Tao's work [61] on round and solid pool fire.

In order to modify air entrainment correlations [61,63,64], researchers have used a series of apparatuses to attain more details about the air entrainment rates [65–68]. For example, Categen et al. [60] and Toner et al. [69] used a hood technique, where products are captured into a hood, to determine the air entrainment rates through mass and species balances. This method has no need for a defining plume boundary. McCaffry [70] used point measurements of temperature and velocity to calculate the mass flux through the plume cross-sections. However, this method omits the density effect and velocity fluctuations important in buoyantly driven flows. In addition, laser doppler velocimetry (LDV) provides the converged statistical information by taking into account the probability density functions of the fire-induced velocity, a way that shows large fluctuations along with radially inward and outward flow patterns. Gore et al. [71] utilized the LDV to measure the velocity field outside the flame boundaries and digital particle velocimetry in order to calculate the entrainment rates. It was found that due to temperature differences, the flame would become swelled and the velocity field moved outwardly; Similarly, the density gradient effect accounts for the formation of vorticity structures and the inward movement. This result confirmed that only a part of the air is carried into the flames to take part in the actual chemical combustion reaction. But the remanent oxidizer that mixes with inert gas (e.g., nitrogen) and combustion products flows through the upper layer, reducing the relative concentrations and temperatures of the flame. In addition, particle imaging velocimetry (PIV), faster than LDV over data processing, was adopted to collect the velocity field data. Zhou [72] used the PIV method to fit the heat release rate and explore the vorticity distributions of the fire-induced flow field. Although results slightly overpredicted the fire-induced velocity field, this method significantly advanced the prediction accuracy.

3.4. Flame height

The visible height above a fire source represents the combustion reactions. Tamanini [73] discussed the manner where the completion of combustion varies with changing flame height. Typically, flame height is thought to combine the luminous part in the lower flaming region appearing fairly steady and the upper flaming region seeming to be intermittent.

In 1983, Heskestad [74] proposed a mathematical correlation for predicting the height of buoyancy-dominated, turbulent diffusion flames, i.e., $\frac{L}{D} = \mathrm{fn}\left(\frac{N}{\alpha}\right)$, where α is the convective fraction of the heat release rate. N represents a dimensionless parameter:

$$N = \frac{c_p T_\infty \dot{m}^2 r^3}{g\rho_\infty^2 H_c D^5} \tag{4}$$

c_p, T_∞, ρ_∞ are the specific heat of air, ambient temperatures, and ambient density, respectively. Further g is the gravity acceleration, $\dot{m}$ is the mass burning rate, r is the stoichiometric mass ratio of air to fuels and H_c is the lower heating value per unit mass. Nevertheless, considering the lip height effect, this expression would be inaccurate when combustion occurs within in-depth pools since a significant volume of oxidized volatiles mix with combustible array by air entrainment. In addition, when assuming that the convection effect is unimportant, one can write the parameter N as:

$$N = \left[\frac{c_p T_\infty}{g\rho_\infty^2 \left(\frac{H_c}{r}\right)^3}\right] \frac{Q^2}{D^5} \tag{5}$$

Q is the heat release rate:

$$\dot{Q} = \dot{m} H_c \tag{6}$$

This modified dimensionless parameter N leds to a satisfying flame height relation:

$$\frac{L}{D} = -1.02 + 15.6 N^{\frac{1}{5}} \tag{7}$$

In 1980, Zukoski et al. [60,75] devoted their seminal works to the measurement of flame height (Fig. 5). They considered the flame intermittency, I, against the flame height above the pool z. The relationship between the intermittency and the distance is defined as "the fraction of time during which a consistent flame lies above a horizontal pool surface up to elevation z." The value of intermittency declining from 1 to smaller values represents the change from the consistent zone to the intermittent or plume zone. The mean flame height L is considered where the intermittency has reached 0.5.

Zukoski [68,75] suggested a new non-dimensional parameter rather than N:

$$Q_{\mathrm{D}}^* = \frac{Q}{\left(\rho_\infty c_{\mathrm{p}} T_\infty \sqrt{gD}\, D^2\right)} \tag{8}$$

and a connection between N and Q_{D}^* is:

$$N = \left[\frac{c_p T_\infty}{\left(\frac{H_c}{r}\right)}\right]^3 Q_{\mathrm{D}}^{*2} \tag{9}$$

Quintiere [76] depicts Q_{D}^* as "chemical energy release rate divided by an effective convective energy transport flow rate due to the buoyant flow associated with length scale D". Seen from below, a formula shows that there are two regions in which flame height varies with burner diameter:

$$\begin{cases} Q_D^* < 1.0, \dfrac{L}{D} = 3.30 Q_D^{\frac{2}{3}} \\ Q_D^* > 1.0, \dfrac{L}{D} = 3.30 Q_D^{\frac{2}{5}} \end{cases} \tag{10}$$

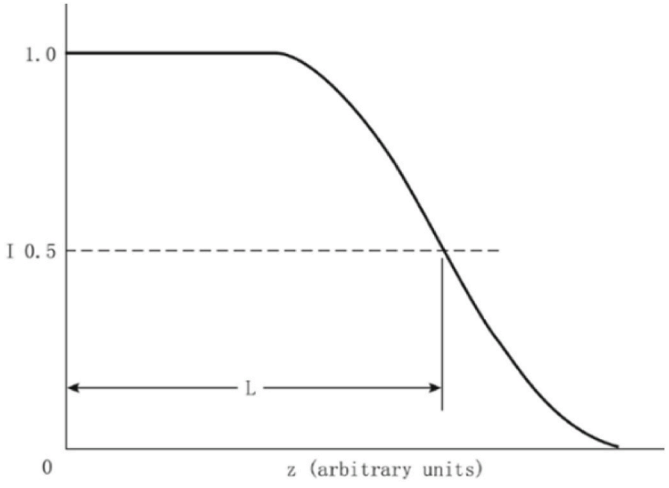

Fig. 5. Definition by Zukosk et al. of mean flame height, from measurements of intermittency, I [75].

The relationship between the flame height and the pool diameter is characterized by the dimensionless heat addition parameter Q_D^*. When the $Q_D^* < 1$, the flame height relies on the pool diameter (D) and is shorter than one-third of the diameter. Moreover, when $Q_D^* > 1$, the flame height is proportional to the two-fifth power of the total heat release rate rather than the pool diameter. Therefore, $Q_D^* = 1$ could be regarded as a meaningful index where the flow conditions (e.g. air entrainment) and the nature of flame combustion change. From $0.1 < Q_D^* < 1$, flame heights vary as $Q_D^{*\frac{2}{3}}$; when the values of Q_D^* are quite small, fires would be segmented into several flamelets, resulting in $L \sim Q_D^{*2}$ [77]. McCaffrey [78] conclude a widely accepted dimensionless flame height equation:

$$\frac{L}{D} = -1.02 + 3.7\left(Q_D^*\right)^{\frac{2}{5}} \tag{11}$$

This expression applies only to standard atmospheric conditions of temperature and components.

Hamins [6,79] stated that both formulas were unsuitable for smoky fires considering the soot concentration and heat feedback effect. He proposed that when χ_a (the actual heat release rate) and χ_c (the convective fraction toward surroundings) were far below 1, the measurement of flame height would deviate from the literature correlations. Additionally, more factors should be considered when one models flame height. For instance, Fig. 6 shows the flame height changes with different oxygen conditions. Chen [35] proposed a new correlation taking into account the effect of oxygen concentration:

$$N^* = \left\{\frac{c_p T_\infty \left[0.233 + 0.204 \times \frac{(1-C_{O_2})}{C_{O_2}}\right]^3}{g\rho_\infty^2}\right\} \times \left\{\frac{r^3_{C_{O_2}=0.21}}{H_c^3}\right\} \times \left\{\frac{Q^2}{D^5}\right\} \tag{12}$$

C_{O_2} is the oxygen concentration, r is the stoichiometric mass ratio of air to fuel under standard atmosphere conditions. The first term on the right-hand side can be seen as an environmental factor involving oxygen concentration; the second term is a fuel parameter; the last term is the fire source parameter, regarded as the controlling factor for surroundings. All in all, when the fuel is burning, the flame height is unsteady with fluctuations; correlations for the flame height usually give average values rather than an accurate result.

3.5. Pulsation & radiation

Many researchers have studied the pulsation phenomenon in pool fire because it affects the burning process and reflects the flow conditions of pool fire [80–82]. The frequency of pulsation was well-fitted by a modified Strouhal number: $St = fD/V$, and Froude number, $Fr = V/(gD)^{1/2}$, which considers the frequency as a function of the inverse root of the source diameter, $f \sim D^{\frac{1}{2}}$. Therefore, frequencies would decline in large pool fires, and the inverse is true. Categen et al. [81,83,84] laid the foundations of the connection between pulsation and vortex structures in pool fire. The pulsation frequency was correlated well in relation to the Strouhal number and Richardson number, a ratio of buoyancy forces to inertia forces $Ri = [(\rho_\infty - \rho_p)gD]/\rho_\infty V^2$. Considering the initial exit velocity of fire, they proposed the frequency relationship by the expression $St = 0.83R_i^{0.83}$ around $Ri < 100$. Meanwhile, their results showed that the formation of the toroidal vortex is initiated by the momentum transfer (buoyant acceleration of light plumes) from axial to radial motion.

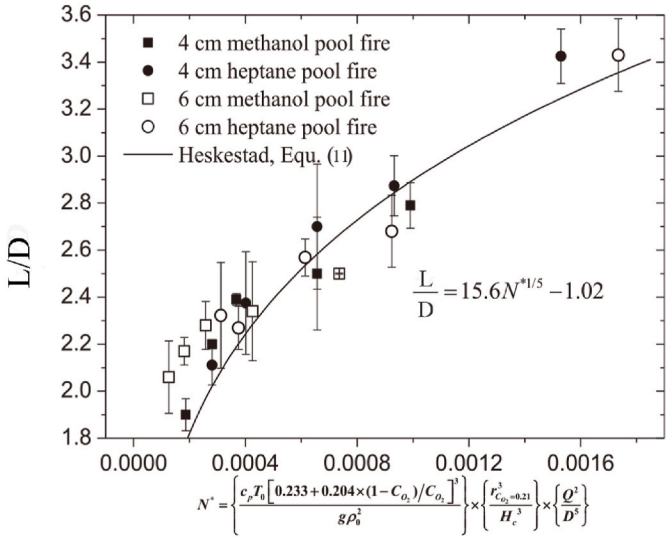

Fig. 6. Flame height data normalized under different oxygen conditions [35].

Additionally, many experimental studies about "puffing" were carried out utilizing various measurement methods, such as hot-wire anemometry, fast photography, acoustic detection, and the Fast Fourier Transform (FFT) technique [85]. Hamins [82] tested the critical fuel velocity needed to initiate the pulsation, suggesting that the fuel exit velocity has a more noticeable effect on flame pulsations than does the heat release rate. In 2000, Categen [83] discussed the instability models of pulsation in buoyant diffusion flames, the first model of which described a sinuous meandering pattern characterized by diffusion flames. This model explains that because diffusion flames contract in the combustion process, the instability gradually evolves into a sinuous motion. The second mode described the varicose flow pattern occurring in the vicinity of the fire source, where toroidal vortical structures form when flame oscillate, causing flame height to fluctuating.

In addition, environmental conditions would influence the pulsation phenomena, e.g. pressure variations. When pressure declines, the amplitude of pulsation increases and thus a portion of the flame would be quenched if the pulsation is so stronger that the combustion process cannot persist [86]. In 2011, Fang [87] investigated the effect of low air pressure and oxygen concentration on pool fire combustion characteristics and pulsation frequency. The pulsation frequency, proportional to the air pressure, is expressed as $f \sim (p^2 g)^{1/3}$ for laminar flames. His results showed that the pool fire was more buoyant in low air pressure than in normal pressure. This pressure effect leads to the more violent periodic oscillation and a higher flame puffing frequency even though the pulsation frequency was mainly thought to be dependent on the size of the pool rather than the fuel property and the burning rate. On the other hand, recent studies found that different aspect ratios of burners and boundary conditions will affect the pulsation behavior, such as sidewall and corner surroundings. Huang [80] considered the hydraulic diameter as the characteristic length scale to modify the pulsation model. The finals showed that convection between the buoyant plume gas and the stagnant surrounds was turbulent and declined when the sidewall and corner appeared. Therefore, the pulsation frequency decreased, in that boundary conditions caused the blockage of air entrainment and the change of the burning model. Based on the mirror approach, Zhang [88,89] proposed global models of flame pulsation involving the effective perimeter of the burner (Fig. 7):

$$f = \begin{cases} 0.53\sqrt{\frac{g}{D_{eff}}} & free\ flames \\ 0.53\sqrt{\frac{g}{D^*_{eff}}} & side\ wall\ and\ corner\ flames \end{cases} \tag{13}$$

D_{eff} is the modified perimeter-equivalent diameter, i.e. $D_{eff} = 2(L + W)]/\pi$; D^*_{eff} is the perimeter-equivalent diameter based on 'mirror' approach considering the effect of air entrainment under different space conditions, it expressed as:

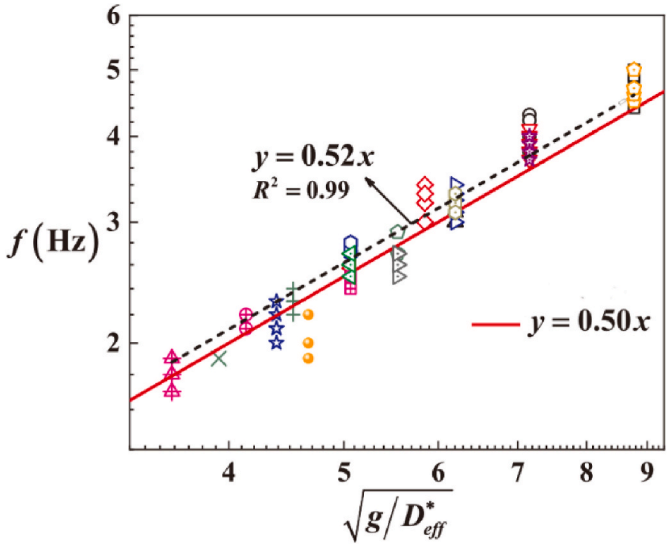

Fig. 7. Pulsation frequency of the free flame model and the modified model treated by the mirror approach and the equivalent diameter [89].

$$D^{*}_{\mathrm{eff}} = \begin{cases} \dfrac{2\cdot W + 2\cdot L}{\pi} & free\ \ flames \\ \dfrac{4\cdot W + 2\cdot L}{\pi} & sidewall\ \ flames \\ \dfrac{4\cdot W + 4\cdot L}{\pi} & corner\ \ flames \end{cases} \tag{14}$$

Radiation plays a critical role in helping transfer heat to evaporate liquid fuels and in ruining adjacent objectives. Some liquid fuels will burn with relatively clear flames compared with those giving a smokier flame. The presence of carbon particles in a pool fire causes some disturbances. One is that the soot will improve the emissivity of the flame, and another one is that the smoke could envelop the flame, reducing radiative output towards surroundings. It was argued [90] that the size of initial carbonaceous particles within the combustion zone of a flame might be governed by residence time at which the large difference of flame structures would occur between smaller and larger fires. In addition, although soot structures depend on the type of fuel, the outcomes of Shaddix et al. [91] proved that the absorptivity of soot only varies slightly with different fuels and flame types, especially for large pool fires. Under large-scale diameters, radiation feedback to the fuel surface can be attenuated from the luminous part of flames because there is a fuel-rich zone with lower temperatures. This reduction, called the radiation blockage phenomenon, will cause the unburned sot particles to be cooler, and then the mass burning rate will fall. The emissions of soot and gas species have been confirmed by employing a mid-infrared spectrometer. Suo Anttila [92] found that for soot-free fuels the dominant emission was from water, carbon dioxide, and the products of combustion. In contrast, the emission of soot dominates carbon-rich fuels. Experimentally, Hamins [93] estimated the flame radiance through a single location measurement method in liquid pool fires. He suggested that the distance of the radiometers should be nearly as five times as the pool diameter from the pool center and at a vertical distance equal to 40% of the flame height. The test results show that radiance intensity is reasonable, and most researchers have accepted this method so far.

Strategies to protect equipment and people from radiation damage depend on how much radiation objectives would receive. One can calculate the thermal radiation received by an external target through the following steps [94]: (1) Determination of geometric characteristics of the pool fire. (2) Determination of average thermal radiation of the flame. (3) Calculation of radiant intensity at a given location. Many measurements of radiation heat loss fraction assume the isotropy condition [95]. Two types of thermal radiation models are widely used in fire engineering calculation, i.e., the point source model and the solid flame model, as can be seen in Fig. 8. The point source thermal radiation model is expressed as:

$$\dot{q}'' = \frac{\dot{Q}_r \cos\theta}{4\pi R^2} \tag{15}$$

and

$$\dot{Q}_r = \chi_R \dot{Q} = (0.21 - 0.0034D)\dot{Q} \tag{16}$$

$\dot{Q}_r$ is the total radiative energy output of the fire, θ is an angle between the normal to the target and the line from source to the target, R is the distance from the point source to the target and χ_R is the radiative fraction. This equation demonstrates a simple relationship varying with the inverse square of the distance R. While neat, it has virtually never been developed as a rigorous method.

The second approach generally used to predict the intensity of thermal radiation is the solid fame radiation model, based on the fact that the radiation stems from the hot products of combustion. The expression is given by the following equation [96]:

$$\dot{q}'' = E_f F \tau \varepsilon_f \tag{17}$$

E_f is the total emissive power of the flame at the fire surface, F is the view factor, τ is atmospheric transmissivity, and ε_f is the emissivity of a flame. The flame is assumed to be a cylindrical, blackbody, homogeneous radiator with average emissive power. The view factor is a function of the target location, the flame diameter and shape. One can find the calculation procedure in radiation books, such as [97].

According to the two classical radiation models, more accurate and complex methods have been proposed to calculate radiation output. Munoz [98] separated a flame into the luminous zone and non-luminous zone by using the superimposition of visible light (VHS) and thermographic camera (IR) images. Based on this way and the solid model, the radiation output can be calculated through the following expressions:

$$E_f = \frac{\eta_{\mathrm{rad}} \dot{m}'' \Delta H_c}{\left(1 + \frac{4L}{D}\right)} \tag{18}$$

The fraction of energy radiated, i.e. η_{rad}, is used to calculate the average emissive power in the cylindrical solid flame model [94]. There is a correlation between η_{rad} and pool diameters, D:

$$\eta_{rad} = \begin{cases} 0.158D^{0.15} & \forall D \le 5\mathrm{m} \\ 0.436D^{-0.58} & \forall D > 5\mathrm{m} \end{cases} \tag{19}$$

This method established how the emissive power, E_f, was disturbed with the assistance of superimposed images to distinguish luminous and non-luminous zone in the pool fire. As a result, it allowed the more accurate calculation of radiative energy received.

Similarly, based on the classical solid flame model, Ji [99] provided a new way to predict the flame emissivity varying with the flame height. A flame was assumed to consist of multiple small cylinders with a diameter of $D(i)$ and a height of Δz. This method takes into account changes in the pool diameter, temperature, and emissivity layer-by-layer to predict the view factors and then radiative heat flux from fire sources. Raj [100] put forward the model about large hydrocarbon fuel fires to predict the variation of thermal radiation along the fire plume and towards the surrounding, including the effect of soot blockage and pulsation. Note that soot forms when there is a lack of enough oxygen in the reaction zone of pool fire and enough fuel concentrations used to supply combustion. For sooty pool fires, the emissive power of large-diameter pools sharply declines by a factor of 6 [101]. The maximum energy is thought to be from the bottom nearly 30% of the flame height [13,102]. Most authors have provided relevant models, including the mean bema length approach combined with the uniform, isothermal, and gray gas absorption approximation. Be that as it may, the non-gray, non-isothermal

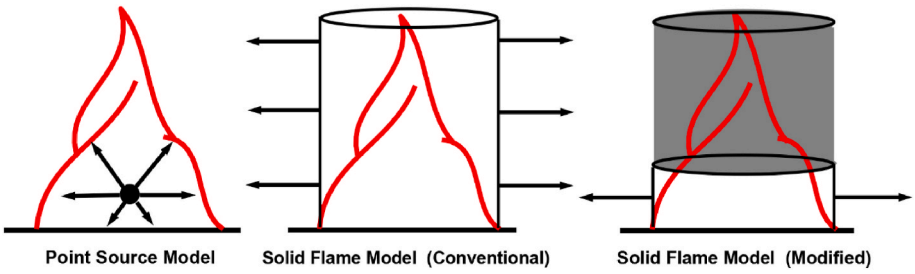

Fig. 8. Schematic diagram of thermal radiation models [96].

and non-homogeneous effects in sooty fires should be considered [103].

Considine [104] considered the emission of LNG fires to draw on the gaseous band emissions and emissions from luminous soot and then provided equations to assess the emissivity related to fire size. Beyler [105] and Moorhous [106] did the same work about LNG pool fires, considering the wind effect and radiant heat hazards. Nevertheless, most of these works did not include the smoke obscuration effect as well as pulsation that affects the flame shape and air entrainment. The formation of dark soot would reduce thermal radiation emission to distant objectives and pool surfaces [6,107,108].

4. Risk assessment of pool fire accidental events

A pool fire stems from the runaway combustion of vapors generated from the flammable liquid when atmospheric or pressurized vessels loss containment, resulting in a steady radiation source [109,110]. Continuous flame radiation and engulfment from a distant fire source would account for the accident escalation of pool fire. Therefore, the continuous degradation of pool fire events, the synergistic effect of multiple pool fires, and the assessment of risk criteria were emphasized in this section as they are explicitly related to pool fire safety.

4.1. Domino propagation trigged by pool fire

Target vessels may be damaged by the engulfment in flames or radiative incidence, thus leading to an escalation. This is generally called the "domino effect". Table 4 illustrates the escalation criteria of pool fire based on the heat load that targets receive [18]. The table shows that the parameters collected are similar to each other in spite of different fire types, which are consistent and stable heat sources and can induce analogous failure mechanisms. It indicatess that a fire risk assessment should involve the escalation for any target vessels inside the pool regime.

When vessels receive steady radiation transfer rather than flame engulfment in the case of pool fire, the possibility of escalation would depend on pool geometry, the thermal properties of the objectives exposed to the fire source, and the radiative intensity. During the evolution of pool fire, Radiation reinforces the propagation of escalation vectors. The greater part of literature has focused on the radiation effect [4,5,111,112] in order to find out what relationships are behind the radiation intensity of pool fire and domino events. In 2015, Spoelstra [113]suggested the inner correlation of safety distance between pool fire radiation and domino effects caused by the pool fire. Fig. 9 shows the distances from the pool edge versus the pool area. And the heat load is regarded as $10kW/m^2$ or $35kW/m^2$ at an observer height of 1 m. The maximum distance was 26 m with a burning pool surface 200 m^2 and the curve fits well. Nevertheless, for the surface area greater than 200 m^2, the outcomes of small distances first displayed an increase and then a decrease in the following distance.

Cozzani [18] comprehensively discussed the pool fire escalation and time to failure (TTF) assessment of atmospheric and pressurized vessels. In his results, it is clear that the second target would be devastated when

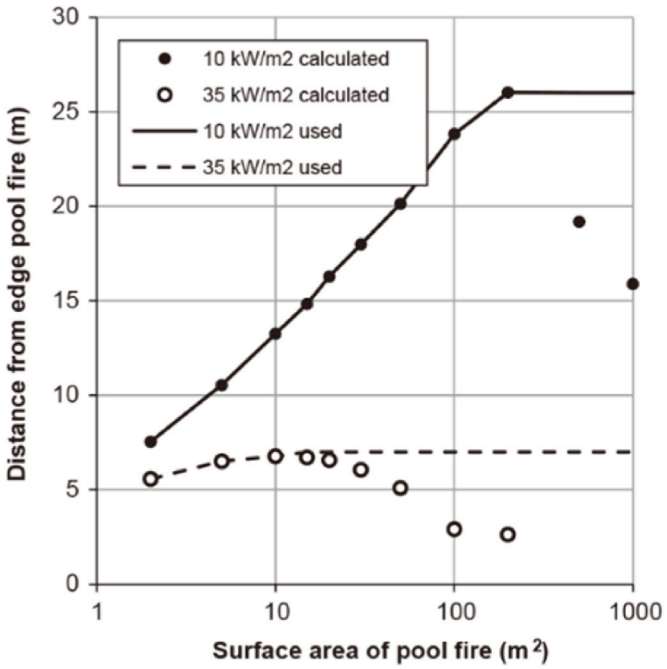

Fig. 9. Pressure vessels' safety distances prevent domino events due to heat radiation from a pool fire [113].

Table 4
Classification of Fires in the process industry.

Features relevant for escalation		Open jet fire	Confined pool/tank fire	Open pool fire	Fireball
Combustion mode		Diffusive	Diffusive	Diffusive	Diffusive
Total heat load (kW/m^2)		100–400	100–250	50–150	150–280
Radiative contribution (%)		50–62.5	92–100	100	100
Convection contribution (%)		37.5–50	0–8	0	0
Flame temperature range (K)		1200–1500	1200–1450	1000–1400	1400–1500
Escalation criteria for fire impingement (kW/m^2)	Atmospheric	Escalation always possible	Escalation always possible	Escalation always possible	Q > 100
	Pressurized				Escalation unlikely
Escalation criteria for distant radiation	Atmospheric	Q > 15	Q > 15	Q > 15	Q > 100
(kW/m^2)	Pressurized	Q > 40	Q > 40	Q > 40	unlikely

considering the escalation for atmospheric vessels at distances lower than 50 m from pool fire. By contrast, a conservative safety distance of 20 m may be adopted for pressurized vessels. Benucci [114] used Fire Dynamics Simulator to calculate the fire hazards of hydrocarbon pool fires. The results were suitable to evaluate the possibility for an individual to survive a fire that entered a safe location and were more accurate than those data obtained from analytical models when obstacles were installed. On the other hand, time to failure is fundamental to risk management and emergency response in fire scenarios. Wu et al. [115] studied the application of time to failure assessment in large crude oil pool fires by simulation method. When protective methods have been used, they would extensively delay the tank failure under the pool fire scenario. Yang [111] discussed the possibility that pool fire alone causes a domino effect through the solid flame model and CFD model. He stressed that although the pool fire can trigger a domino event, the domino accident is nearly unlikely to occur when a safety distance is settled.

For chemical and process complexes, pool fires not only generate energy that feeds back to the burning surface, but also emit radiative heat flux that would ignite adjacent liquid fuels and objectives. It is commonly assumed that the radiation intensity is in inverse proportion to the square of interval distance [116] but this intensity is also influenced by pool diameters and the interval distance between objectives. In order to understand how pool fire threatens nearby liquid fuels, two parameters are investigated in this context, i.e. fireproofing distance and ignition time.

In recent years many researchers have attempted to accurately predict radiation output and thus define satisfactory fireproofing distance [7,115,117,118]. Wu et al. [119], for instance, suggested that the distance should be larger than 0.4 times the diameter of oil tanks through FDS simulation. Li et al. [120] studied the distant ignition of combustible liquid fuels by measuring radiative emission from adjacent pool fire. In their study, critical ignition distance and critical ignition time were measured. Critical ignition distance is defined as the maximum distance at which targets can be ignited in the vicinity of other fire sources; Moreover, critical radiant heat flux is the minimum radiant heat flux that adjacent liquid fuel receives to cause ignition. Considering the cylindrical model for radiation transfer, they found that for fuels with lower flashpoints, the critical ignition distance is larger than that of those with higher flashpoints, while the former needs less energy for ignition. And they found that ignition time has a weak relationship with pool diameter; however, the ignition time leaps significantly with an increase in interval distances due to the fact that radiative heat flux was attenuated.

Wan et al. [121] made an important contribution with regard to the impact of flame shape and radiation distribution. Instead of using traditional radiation models, as discussed in Section 3.5, they proposed a multi-point source model by defining the weight of each point source and flame volume fraction. The result showed that the radiation heat flux received by adjacent pools tallied well with values from Chinese standards. According to the final calculated results, although the treatment did not consider the tilting and trailing of flames, their model can provide an acceptable safety distance for people and liquid pools exposed to fire sources. Hence, the result is conservative and limited to wind-free conditions.

4.2. The impact of multiple pool fires

In chemical and process industries, multiple pool fire sources would occur and their radiation output is more intensive than that of a single fire source [5,122], posing a serious threat to adjacent people and facilities. It has shown that the characteristics of multiple pool fires are significantly different from those of a single pool fire. Many analyses have been carried out to assess potential hazards involving the interaction of multiple pool sources [10,123–125]. For a single pool fire, the heat release rate is controlled by the heat feedback from flames to support the evaporation of the liquid fuel. By contrast, for multiple pool fires (MPF) the interactions of fire would cause more serious disturbances on both the heat feedback and air flow in the combustion regions (temperature rise), resulting in an increase in flame height and different burning behavior, such as fire whirl [125]. Hence, it is of interest to introduce the multiple pool fire effect in fire safety terms.

In realistic urban and chemical process fires, a question is whether one group of fire points would act as the initial source to induce another fire propagation or whether new fire sources would reversely act on tanks by synergistic effect. Liu [125,126] investigated the spatial distributions of multiple pool fires and their mass burning rates, suggesting that the physical mechanism of heat feedback was enhanced and air entrainment was restricted. For multiple pool fire sources, the high competition between two effects, i.e. heat feedback and air entrainment restriction, cause fluctuations in mass burning rates. And both effects are further affected by the fire spacing and fire array size. Hence, this result would be significant as the heat release rate depends on mass burning rates, and discrete fuel sources are mainly ignited by radiation and firebrands [19]. Pantousa [127] numerically studied the structural integrity of tanks affected by multiple pool fire scenarios. Fig. 10 shows that the target tanks were subject to non-uniform radiation generated by adjacent fire-engulfed tanks. Relying on the solid flame model, he denoted that fire resistance changes nonlinearly with the increase in burning tanks because multiple fire sources widen heated zones, leading to complicated temperature distribution. Similar work was implemented by Sengupta [128], who investigated the layout of fuel tanks and the effect of multiple pool fires after ignition. Cozzani [19] pointed out that the conventional risk models are not suitable for analyzing the consequences of multiple pool fires because a detailed assessment of multiple contemporary fire events is too difficult to afford. Nevertheless, he suggested that the accident consequences may be analyzed by superimposing physical effects (radiation, pressure, flame height) and neglecting the synergetic effects, a way that would enlarge uncertainty in risk assessment.

4.3. Societal & individual risk criteria

A full fire risk assessment should estimate the incidence and subsequent consequences of hazardous scenarios, an assessment that is related to individual and societal risks. In the context of pool fire, the plotting of individual and societal risks may be changeable since the burning conditions of pool fire are ‘non-fixed’. It appears that introducing the concept of risk criteria would be relevant to this study, given that both individual and societal risk could directly depict a risk level of pool fire [129].

Individual risk to the public may be expressed as a function of distance from the fire source, but it is more generally taken as the average risk to people at different areas around the source. The HSE [130] proposed that an ‘intolerable’ fatality risk is 10^{-3}/year (the frequency of individual fatality per year), while a ‘broadly acceptable’ fatality risk is shown as 10^{-6}/year. The risk of an individual is formulated in simple ways as [131]:

$$r_{ir} = \frac{1}{N}\sum_{i=1}^{n} x_i f_i \tag{21}$$

f_i is the frequency of an accident type i, r_{ir} is the individual risk of death, x_i is the number of deaths for corresponding accidents, n is the number of accidental types, and last N is the total numbers of people at potential risk. In addition, the main form of societal risk is presented as a relation between the death toll of incidents, N, and the frequency F of such incidents. Estimation of societal risk involves the determination of populations at risk. These data may be finally displayed in tabular form or plotted as an FN curve or risk contours on a map. Each phase of the assessment is accompanied by uncertainty. For instance, using Aripar-GIS software, Cozzani [19,132] studied the individual and societal

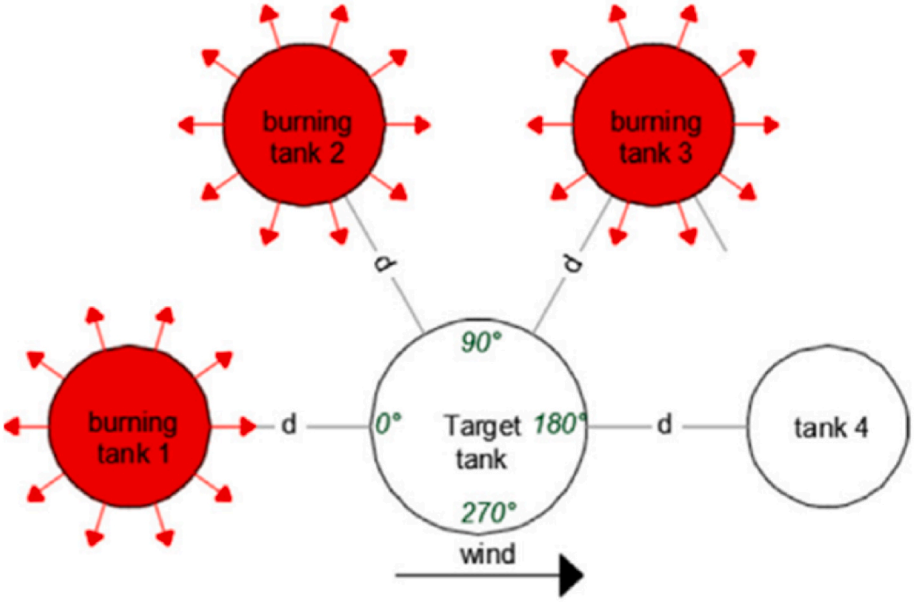

Fig. 10. Layout of multiple fire scenarios [127].

risks with domino effects that were initiated by pool fire in the chemical process. When the propagation of pool fire and domino effects were considered, the individual risk was significantly higher than that of the original results without modification. And for F–N curves, the societal risk showed lower expected frequencies but a higher expected death toll.

These risk criteria are intended to be used in conjunction with a fire risk assessment. Although both individual and societal risks only express the potential losses of objectives that are regarded as points in the fire events, experts concerning different pool fire conditions would provide more reasonable decisions when using these statistical ways.

5. Discussion

5.1. Heat feedback analysis for controlling the mass burning rate

Mass burning rate per unit area increases with pool diameters up to 2–3 m, above which, however, the rate would be independent of diameter or may decrease slightly [32,133]. This change occurs because soot products increase and radiation loss toward outside growths, resulting in the fire to be optically thick and saturated. This mass burning rate would also be affected by several factors, such as fuels with the lowest heat of gasification and pools with different initial temperatures. The mass burning rate of liquid pool fire is generally predicted by fire models concerning heat balance and heat feedback effects. The heat transfer model is reciprocally affected by the diameter of pools. For small pool fires, heat conduction from the pool rim will be large, and then the mass burning rate will be high, whereas for large pools the conduction effect can be negligible. Radiation heat transfer will be dominant with increasing pool diameters as there is a large and nearly constant value of the term $1 - \exp(-k_4 D)$. If the pan size is intermediate, the heat conduction will again be negligible, and the radiation will not be significant due to the optical thin of a flame. As can be seen in Table 5, the burning model is characterized by conduction or convection when the diameter is less than $0.2m$. When combustion starts, the flow pattern can be laminar or turbulent in the convective regime and pool fire will be radiation-dominated if $D > 0.2m$. Further, when the pool diameter is above 1 m, the radiation in Eq. (1) dominates the heat transfer to the pool surface. It might indicate that the pool fire becomes a large, optically thick, and radiating black body. In addition to the size effect, vessels made of different materials would also cause the perturbations of mass burning rate, mainly due to changes in conductivity [134].

Table 5
The burning regimes for liquid pools.

Diameter (m)	Burning mode
<0.05	Conduction, convective, laminar
0.05–0.2	Convective, turbulent
0.2–1.0	Radiative, optically thin
>1.0	Radiative, optically thick

Similar work on the mass burning rates of solid plastic fuels was investigated by de Ris [102], including polymethylmethacrylate (PMMA), polypropylene (PP), and polystyrene (PS). He found that the fuel type seems to be irrelevant to the actual heat release rate. An explanation was given by the fact that for most organic fuels, the oxygen consumed per unit mass releases nearly identical heat energy despite incomplete combustion. Although oxygen consumption is controlled by the turbulent mixing rate, the mixing process driven by temperature differences is generally insensitive to the fuel. On the other hand, increasing lip height can affect the temperature distribution around the wall of fuel vessels and thus can change the heat transfer efficiency by conduction. Lip height can promote the turbulence of pool fire and improve heat transfer by convection, while on the base of the pool, the flame would be more stable and emissive. Kuang's work [135] proved previous inferences by experiment and simulation methods that when vessels have large lip height, the mass burning rate of pool fire will first decrease and then increases, and the reverse is true.

5.2. Underlying mechanisms for pressure and boilover phenomena

Lower pressure at high altitudes will influence the burning characteristics of pool fire, complicating the risk assessment process. From the fire modeling perspective of view, one can conclude $K_s \sim p^2$ and $L_m = \frac{3.6V_f}{A_f} \sim 0.9D$ [136]. And the mass burning rate under lower pressure could be expressed as $\dot{m}'' \sim \sigma T_f^4[1 - \exp(-\kappa_s L_m)]/\Delta H_g$, which can be treated by the expansion of exponential method: $\dot{m}'' \sim 1 - (1 - \kappa_s L_m) \sim \kappa_s L_m$; then it follows that [40]: $\dot{m}'' \sim \kappa_s L \sim p^{3/2} {L_m}^{3/4}$. This scaling law demonstrates the cause-and-effect relationship between burning rate and pressure for the radiation-controlled pool fire. As can

be seen in Fig. 11, the overall correlation of pressure effects is recapitulated as follows:

$$\dot{m}'' \propto \dot{p}^{n}, n \approx \begin{cases} < 0, conduction \\ 0 \sim 1, transition \\ 1 \sim 2, convection \\ 1 \sim 1.7, radiation \end{cases} \quad (22)$$

Under lower pressure, the flame height would be slightly higher than that under normal pressure. When pressure is reduced, the air density falls. This change will result in a smaller air entrainment flow rate [43,137], meaning the flame requires longer entrainment paths. Generally, at high altitudes the burning rate would decrease as well as the number of soot particles [41]. By contrast, the mass burning rate and the radiation loss would rise with an increase in pressure because more soot particles are produced; the flame will convert from laminar to turbulent, and its color changes from blue to yellow [44].

Boilover happens when the vapor pressure sufficiently overcomes the head of liquid above. This burning process will eject burning oil aided by explosive water vaporization. When the uniform temperature distribution does not form and the "hot zone" propagation velocity is greater than the surface regression velocity, the danger would occur with large storage tanks containing these liquids. Table 6 shows the comparison between the descent rate of the hot zone and the regression rate. The underlying principle of hot zone formation has not been proposed, but this phenomenon is exclusively related to fuel mixtures. The water near the bottom of the fuel may be kept in a superheated state. Thus, bubbles may form at the interface because of ebullition, causing a rapid increase in temperature in the fuel layer. When bubbles pass through the fuel layer, it induces a furious stirring effect that fluctuates interfacial temperatures between the fuel and water layer. It seems that water undergoing "boiling nucleation" is a key procedure [53,138]. When the fuel thickness is small, the water would be regarded as a heat sink, and the burning rate, meanwhile, dropped.

5.3. Air entrainment

Air entrainment is induced by the buoyant force that continuously triggers the ascent of hot gases replaced by the cold ambient, supplying the oxidizer for fuel combustion. Entrainment rates of air surrounding a fire plume are critical to estimating fire spread and burning rates in various fire accident scenarios because the rates would change flame shape, partial premixing, soot formation, radiation emission, and fuel consumption.

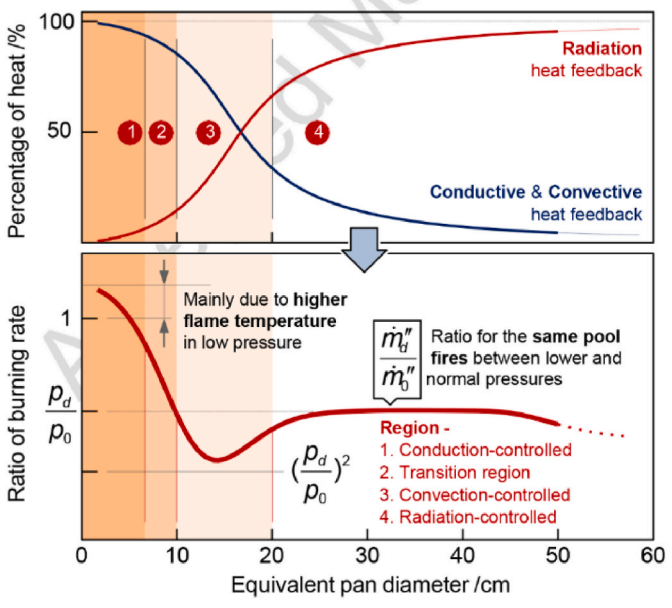

Fig. 11. The graphic analysis of pressure effects on the mass burning rate and different heat feedback mechanisms [40].

Table 6
Comparison between rates of propagation of hot zones and regression rates of liquid fuels [139].

Oil type	Rate of descent of hot zone (mm/min)	Regression rate (mm/min)
Light crude oil		
<0.3% water	7–15	1.7–7.5
>0.3% water	7.5–20	1.7–7.5
Heavy crude and fuel oils		
<0.3% water	up to 8	1.3–2.2
>0.3% water	3–20	1.3–2.3
Tops (light fraction of crude oil)	4.2–5.8	2.5–4.2

Air entrainment is difficult to accurately calculate because it is extremely sensitive to spatial distribution and vessels' geometry. Most of the air entrainment models are based on two simplified assumptions: (1) the velocity and temperature are constant on the cross-section of a flame; (2) the flame is cylinder-shaped, and its diameter is equal to the size of the burner. A representative is a top-hat profile model, which states that the amount of air entrained into the flame can be calculated by regarding that the vertical mass flow rate at every height where combustion occurs is equal to the number of vaporized fuels plus the air entrained at the current height. While the 'top-hat' assumption simplifies the calculation procedure of air entrainment, this method would show slightly tapered shapes under small or medium diameters (i.e., $D < 2m$) rather than almost cylindrical shapes for large fires. Additionally, some dimensionless parameters are frequently used to characterize the flow state, for example, Reynolds number, Rayleigh number, Grashof number, and Froude number. Froude number is the ratio of inertial forces to the buoyant forces, $Fr = \frac{u^2}{gL}$; When it is far below 1, the entrainment mechanism is dominated by buoyancy, and therefore the dimensionless flame height L/D can be estimated with Fr [17].

5.4. Analysis of flame height assessment

Flame height displays how the fuels evaporated interact with surroundings or whether the combustion reactions are primarily complete or the inert plume is thought to begin. It is also a key parameter in calculating radiative heat transfer to objects away from the fire sources since the shape and height of fires have enormous implications for fire hazards. These objectives might be ignited by the accumulated heat to cause consequential damage or domino phenomena. Thus, from a risk assessment point of view, accurately predicting flame height is helpful in investigating the combustion states and safety distances [140].

The shape of pool fires can be divided into three regions: (1) the fuel-rich core zone, where flame height is persistent; (2) An intermittent region, where the flame height varies with time; (3) a downstream plume region [141]. The plume zone can be regarded as non-reacting while the majority of the combustion processes occur in the intermittent zone, and there is a fuel-rich core, the length of which nearly stands at 20% of the global flame height. These regions are relatively cool and full of intermediate products, and their combustion states gradually change with the height from laminar, buoyancy-controlled to turbulent conditions. According to previous investigations, although Q^*_D had been used extensively and successfully, Heskestad [142] pointed out that a number of experiments show that this parameter does not delineate correctly for changes in the ambient temperature, whereas the former scaling parameter, N, counts. One may be interested in why the parameter N is better than Q^*_D when both of them are used to fit the flame height under different ambient temperatures. Heskestad concluded that Q^*_D was simply assumed to use in the combustion region. Recalling that there are primarily three regions in the visible flame

height. When the temperatures fluctuate, such as in a high ambient temperature, the Q_D^* formulation does not sensitive to this effect so the calculated flame height will be different from the values observed.

5.5. Pulsation & radiation transfer

Pulsation predominately impacts the burning process, a movement that supports extra oxygen into the reaction zone for combustion and soot formation. If flame boundaries start oscillating near the source of a pool fire, a number of toroidal vortical structures will form, which rise through the main flame body. This process will influence the mass burning rate and thus change flame characteristics, such as entrainment, flame height, and radiation. Meanwhile, pulsation is associated with the instability of the buoyant flow in the burning process. The instability affects how combustion products periodically form large vortices that push air into the reaction zone and cause the combustion gases to accelerate to create characteristic necking profiles. It is observed that there is a continuous cycle of expansion and contraction of flame height through the structures rising and burning out. Zukoski et al. [143] and Hamins [6] found that when pool diameters were fixed, the lower heat release rates or flame heights, the stronger the magnitude of intermittency would happen.

Thermal radiation can damage the environment and other equipment, such as storage tanks in the vicinity of the fire source, resulting in significant increases in fire accidents and property loss. The hazard of thermal radiation from pool fires is mainly attributed to the fuel type and the fire size, namely, the composition of fuels, the physical dimensions, and the duration of the flame [144,145]. Radiation is closely linked with soot productions because it is influenced by the emissivity of soot. Many researchers have discussed the mechanism of soot formation [146–148]. Briefly, two physical phenomena can explain the formation of smoke. The first is the lack of enough oxygen in the fuel-rich zone within the flame to support the burning of carbon produced by the pyrolysis of the fuel gas. And the second is due to the formation of vortex structures, which bring the air into the flame, a process that lower the core temperature of the fire. Radiation heat transfer from the flame to the fuel surfaces is the dominant heat feedback mechanism in medium and large fires ($D > 0.3m$) and controls how fast liquid fuels evaporate. In addition to the radiation from flames to the pool surface, another key point that most fire engineers care about is the magnitude of radiative energy reaching external targets.

The classic methods to calculate radiative energy include the point source model and the solid model. The use of the point model is limited because it would overestimate the intensity of thermal radiation incident on the target, an overestimation brought about the fact that the radiation in the near-field is mainly affected by the flame size, shape, and soot. The result of the point source method is considered conservative within a few fire diameters as it assumes that all of the radiation energy is emitted at a single point rather than one distributed uniformly (a cone or cylinder). Moreover, for the solid model determining the emissive power E is problematic because it relates to a variety of gaseous species, such as water vapor, carbon dioxide, and luminous soot particles. The theories of gas radiation and the relevant models describing the band emission can be found in Ref. [149]. During pool fire experiments, a substantial portion of the flame is obscured by thick black smoke. This smoky layer would absorb the amount of radiation and reduce the emission to the surroundings. As a result, the prediction of the emissive power of a large fire is subject to a significant error.

5.6. Relationships between fire risks and pool fire characteristics

In industrial fire protection, a major challenge is to regulate the unsteady, open pool fire in which thermal radiation is the dominant mechanism for damage to adjacent property. When the burning of pool fire deviates from normal conditions, this will consequentially alter and complex fire risk assessment. Recalling in Fig. 9, radiative energy does not monotonously increase although pool diameters keep rising, suggesting that the safety distance could be shorter than people previously expected. This trend can be explained by radiation blockage and flame obstruction effects. When the pool fire area increase, more energy is radiated to the surroundings and thus leads to longer safety distances. Note that for larger pool fires, conversely, burning would be more inefficient and consequently produce a substantial amount of soot that shrouds flames and absorbs radiation energy [150,151]. The obscuration of flames explains why distances can decrease beyond a critical value of pool diameters.

The radiative hazards from pool fire depend on numerous parameters, including the fuel types, the diameter and shape of a pool, the soot production of combustion, and the thermal characteristics of the goal receiving incident radiation. Previously, the calculation of radiation transfer has been discussed, and the radiation model generally regards pool fire as a solid, cylindrical-shaped gray emitter. Geometrically, the dimension of the flame area is represented by the flame base diameter and the visible flame height; Meanwhile, both parameters are dependent on the pool size and the burning rate. In reality, the burning behavior of a large pool fire is significantly distinct from smaller flames. Compared with the predicted radiation, the radiative output of pool fire is not uniform for a given flame surface zone that is described by the flame height and the pool diameter.

Figs. 12 and 13 show the average emission of pool fires as a function of the height normalized by the pool diameter and compare the measured and calculated radiative heat flux from pool fire. For the estimation, the average is determined over a radial distance which would be less than the pool diameter because of the necking effect. This distribution in the graph would remind us that the approximations are made in determining the flame shape, height, and corresponding emissive energy over that flame shape. While useful formalism, these methods used to find the emissive power would be somewhat considered empirical, giving similarities with experimental measurements at a distance. Hence, one should be more cautious about evaluation processes and understand the potential disturbance between the unsteady burning conditions of pool fire and risk assessment results.

All in all, fire risk assessment mainly considers the radiation transfer in pool fire events in chemical and process industries. On the basis of this consideration, fire experts can calculate the time to lose containment and set fire safety distance, fire protector and others. However, if one can combine the risk assessment methods and the effects of physical changes on pool fire burning, it would be better to meet the need for assessing how pool fire evolves under complex circumstances (such as environment or geometrical changes). In that case, experts will provide a more global and accurate evaluation of pool fire accidents.

6. Conclusion & future challenges

Pool fire has been thoroughly studied for decades. The investigation of pool fire not only helps researchers know how pool fire evolves during

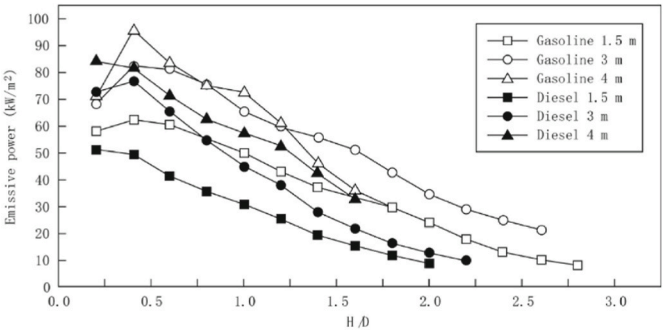

Fig. 12. Emissive power averaged over the measured flame width as a function of the nondimensional height above the pool surface [152].

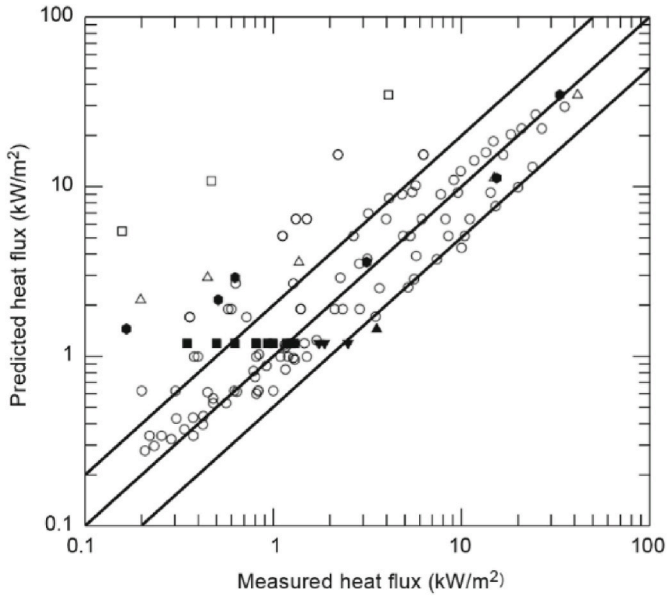

Fig. 13. Comparison of measured and calculated radiative heat flux, solid lines indicate the equality of relevant heat fluxes [153].

combustion, but also lets them decide how chemical and process industries should contain the escalation of dangerous fire scenarios. When pool fire occurs, there are many factors that affect the burning behavior of pool fire, ranging from environmental conditions (e.g. pressure) to spatial distribution (e.g. interval distances between objectives). Therefore, the final risk assessment of pool fire could deviate from that under standard conditions. And it should be noted that although pool fire is usually large in reality, researchers have successfully gained many insights into pool fire and its protection by using small or medium-scale pools. According to previous literature, several aspects can be concluded.

1. Mass burning rate is one of the most important parameters in pool fire and controlled by the heat feedback from flames to liquid fuel surfaces, a process that can be represented by the heat balance equation. This burning rate is related to the scale effect and changes nonlinearly with the increase in pool diameters. When pool fire is radiation-controlled and optically thick, the mass burning rate is under the control of soot products and radiation transfer, where the term $1-\exp(-k_4 D)$ is dominant in the pool fire feedback loop and nearly constant. In addition, the mass burning rate of pool fire is sensitive to different environmental conditions. Under higher altitudes, the lower pressure will slow the mass burning rate since, according to Tu's model $\dot{m}'' \sim \kappa_S L \sim p^{3/2} L^{3/4}$, the mass burning rate is directly proportional to pressure and pool length scale. Similar to the effect of pressure on mass burning rate, flame height under different ambient oxygen concentrations can be fitted with a new dimensionless parameter N^* (Section 3.4), which gives more accurate results than those from Heskestad's equation. And pulsation phenomena of pool fire near a wall or corner can be calculated using Zhang's model, which is based on the mirror approach and considers air entrainment. However, previous research is based on small scales. When a larger pool fire is combined with different initial conditions (pressure, ambient temperature, etc.), the burning behavior is more complex. For instance, for a large pool fire, the fuel-rich core would significantly attenuate the radiative feedback, and this vapor core will be different under high latitude due to lower pressure and oxygen. The synergistic effect of these parameters would cause unacceptable uncertainty in fire safety distances for larger pool fire. In this context, the underlying principles of large pool fire remain to be seen. Numerical methods would be a way out.
2. In the process of combustion, Air entrainment is induced by the buoyant force and influences the flame height and soot formation. Air entrained into the flame supports the burning, leading to the pulsation behavior and lowering the inner temperature of the flame. In turn, when flame pulsates, vortex structures will form and thus accelerate the combustion. In practice, these parameters would be influenced by pool geometry or whether the pool is surrounded by other objectives. This influence would be important to the ignition of adjacent liquid fuels and to how to design a reasonable spatial distribution. Thus, much work should be done with respect to the burning behavior that is subject to barriers.
3. Multiple pool fire sources would occur, which cause different burning mechanisms and would lead to more serious domino events in chemical and process industries. It is observed that there is a furious competition of heat feedback among multiple pool fires, and that air entrainment is restricted by unsteady flow conditions. In this context, fire risk assessment, including individual and societal criteria, is disturbed. Thus, it is necessary to ascertain how multiple pool fires evolve over a large scale and how their radiation output influences risk assessment results.

It should be noted that computational fire modeling is essential for contemporary fire safety control, and this modeling requires high-quality data input. Given that most experiments were implemented under a laboratory scale, there still lacks data on large hydrocarbon fires in relation to radiative fraction, heat feedback, CO, and soot yields to validate fire models.

Declaration of competing interest

The authors declare that they have no known competing financial interests or personal relationships that could have appeared to influence the work reported in this paper.

Data availability

No data was used for the research described in the article.

Acknowledgements

This work was supported by the National Natural Science Foundation of China (CN) [No. 51874255, No. 52174209]. The authors are very grateful to Guoqing Xiao, Lingyuan Wnag, Chao Chen, and Anthony Hamins for their valuable discussions of this paper.

References

[1] E. Planas-Cuchi, H. Montiel, J. Casal, A survey of the origin, type and consequences of fire accidents in process plants and in the transportation of hazardous materials, Process Saf. Environ. Protect. 75 (1997) 3–8.
[2] P. Joulain, Convective and radiative transport in pool and wall fires: 20 years of research in Poitiers, Fire Saf. J. 26 (1996) 99–149.
[3] B.R. Morton*, F.R.S. Sgt, J.S. Turner, Turbulent Gravitational Convection from Maintained and Instantaneous Sources, Proceedings of the Royal Society of London. Series A. Mathematical and Physical Sciences, 1955, pp. 1–23.
[4] F. Kadri, E. Chatelet, G. Chen, Method for quantitative assessment of the domino effect in industrial sites, Process Saf. Environ. Protect. 91 (2013) 452–462.
[5] G. Landucci, G. Gubinelli, G. Antonioni, V. Cozzani, The assessment of the damage probability of storage tanks in domino events triggered by fire, Accid. Anal. Prev. 41 (2009) 1206–1215.
[6] A. Hamins Kt, R.R. Buch, Characteristics of Pool Fire Burning, Fire Resistance of Industrial Fluids, ASTM International, 1996, pp. 15–41.
[7] C. Gong, L. Ding, H. Wan, J. Ji, Z. Gao, L. Yu, Spatial temperature distribution of rectangular n-heptane pool fires with different aspect ratios and heat fluxes received by adjacent horizontal targets, Fire Saf. J. 112 (2020).
[8] X. Zhang, L. Hu, L. Wu, L.W. Kostiuk, Flame radiation emission from pool fires under the influence of cross airflow and ambient pressure, Combust. Flame 202 (2019) 243–251.

[9] F.T. Longhua Hu, Q. Wang, Z. Qiu, Burning characteristics of conduction-controlled rectangular hydrocarbon pool fires in a reduced pressure atmosphere at high altitude in Tibet, Fuel 111 (2013) 298–304.
[10] A. Yip, J.B. Haelssig, M.J. Pegg, Multicomponent pool fires: trends in burning rate, flame height, and flame temperature, Fuel (2021) 284.
[11] D. Kong, Z. Zhang, P. Ping, X. He, H. Yang, Effects of the initial fuel temperature on burning behavior of crude oil pool fire in ice cavities, Exp. Heat Tran. 31 (2018) 436–449.
[12] S.-X.L. Bing Chen, Chang-Hai Li, Quan-Sheng Kang, Vivien Lecoustre, Initial fuel temperature effects on burning rate of pool fire, J. Hazard Mater. 188 (2011) 369–374.
[13] K.S. Jian Chen, Zhigang Wang, Wai Cheong Tam, Ki Yong Lee, Hamins Anthony, The evolving temperature field in a 1-m methanol pool fire, J. Fire Sci. 39 (2021) 309–323.
[14] Y. Lin, L. Hu, X. Zhang, Y. Chen, Experimental study of pool fire behaviors with nearby inclined surface under cross flow, Process Saf. Environ. Protect. 148 (2021) 93–103.
[15] X. Zhang, X. Zhang, L. Hu, R. Tu, M.A. Delichatsios, An experimental investigation and scaling analysis on flame sag of pool fire in cross flow, Fuel 241 (2019) 845–850.
[16] L. Hu, J. Hu, S. Liu, W. Tang, X. Zhang, Evolution of heat feedback in medium pool fires with cross air flow and scaling of mass burning flux by a stagnant layer theory solution, Proc. Combust. Inst. 35 (2015) 2511–2518.
[17] P.K. Raj, LNG fires: a review of experimental results, models and hazard prediction challenges, J. Hazard Mater. 140 (2007) 444–464.
[18] V. Cozzani, G. Gubinelli, E. Salzano, Escalation thresholds in the assessment of domino accidental events, J. Hazard Mater. 129 (2006) 1–21.
[19] V. Cozzani, G. Gubinelli, G. Antonioni, G. Spadoni, S. Zanelli, The assessment of risk caused by domino effect in quantitative area risk analysis, J. Hazard Mater. 127 (2005) 14–30.
[20] L. Hu, A review of physics and correlations of pool fire behaviour in wind and future challenges, Fire Saf. J. 91 (2017) 41–55.
[21] P. Joulain, The Behavior of Pool Fires: State of the Art and New Insights, Twenty-Seventh Symposium (International), 27, on Combustion/The Combustion Institute, 1998, pp. 2691–2706.
[22] D. Evans, Database searches for qualitative research, J. Med. Libr. Assoc. 90 (2002) 290.
[23] B.D. Ditch, J.L. de Ris, T.K. Blanchat, M. Chaos, R.G. Bill, S.B. Dorofeev, Pool fires – an empirical correlation, Combust. Flame 160 (2013) 2964–2974.
[24] A. Nakakuki, Heat transfer in small scale pool fires, Combust. Flame 96 (1994) 311–324.
[25] F. Liu, J.-L. Consalvi, P.J. Coelho, F. Andre, M. Gu, V. Solovjov, B.W. Webb, The impact of radiative heat transfer in combustion processes and its modeling – with a focus on turbulent flames, Fuel (2020) 281.
[26] V.I. Blinov Gnk, Diffusion Burning of Liquids, Army Engineer Research and Development Labs Fort Belvoir VA, 1961.
[27] H.C. Hottel, 'Review: certain laws governing the diffusive burning of liquids', by Blinov and Khudiakov (1957) (Dokl. Akad. Nauk SSSR, 113, 1096), Fire Res. Abstr. Rev. 1 (1959) 41–43.
[28] K. Akita Ty, Heat transfer in small pools and rates of burning of liquid methanol, Symp. (Int.) Combust. 10 (1965) 943–948.
[29] A. Hamins, Energetics of Small and Moderate-Scale Gaseous Pool Fires, NIST Technical Note 1926, National Institute of Standards and Technology, Gaithersburg, MD, October 2016.
[30] A. Shinotake Sk, K. Akita, An experimental study of radiative properties of pool fires of an intermediate scale, Combust. Sci. Technol. 43 (1985) 85–97.
[31] X. Tian, C. Liu, M. Zhong, C. Shi, Experimental study and theoretical analysis on influencing factors of burning rate of methanol pool fire, Fuel (2020) 269.
[32] V. Babrauskas, Estimating large pool fire burning rates, Fire Technol. 19 (1983) 251–261.
[33] A. Nasr, n Ss, H. El-Rabii, J.P. Garo, L. Gay, L. Rigollet, Heat feedback to the fuel surface of a pool fire in an enclosure, Fire Saf. J. 60 (2013) 56–63.
[34] J. Stephen, B.H.-D. Fischer, William L. Grosshandler, The structure and radiation of an ethanol pool fire, Combust. Flame 70 (1987) 291–306.
[35] J. Chen, X. Zhang, Y. Zhao, Y. Bi, C. Li, S. Lu, Oxygen concentration effects on the burning behavior of small scale pool fires, Fuel 247 (2019) 378–385.
[36] Dougal Drysdale, An Introduction to Fire Dynamics, John wiley & sons, 2011.
[37] L. John, DE RIS PKWaGH, Radiation fire modeling, Proc. Combust. Inst. 28 (2000) 2751–2759.
[38] J.G. Quintiere Bsg, A Unified Analysis for Fire Plumes, 27, Twenty-Seventh Symposium (International) on Combustion/The Combustion Institute, 1998, pp. 2757–2766.
[39] R.L. Alpert, Pressure modeling of fires controlled by radiation, Symp. (Int.) Combust. 16 (1977) 1489–1500.
[40] R. Tu, Y. Zeng, J. Fang, Y. Zhang, Low air pressure effects on burning rates of ethanol and n-heptane pool fires under various feedback mechanisms of heat, Appl. Therm. Eng. 99 (2016) 545–549.
[41] R. Tu, J. Fang, Y.-M. Zhang, J. Zhang, Y. Zeng, Effects of low air pressure on radiation-controlled rectangular ethanol and n-heptane pool fires, Proc. Combust. Inst. 34 (2013) 2591–2598.
[42] M. Baki, T.A.A. Cetegen, Experiments on the periodic instability of buoyant plumes and pool fires, Combust. Flame 93 (1993) 157–184.
[43] F. Tang, K. Zhu, M. Dong, Q. Shi, Mean flame height and radiative heat flux characteristic of medium scale rectangular thermal buoyancy source with different aspect ratios in a sub-atmospheric pressure, Int. J. Heat Mass Tran. 84 (2015) 427–432.
[44] J. Chen, Y. Zhao, X. Chen, C. Li, S. Lu, Effect of pressure on the heat transfer and flame characteristics of small-scale ethanol pool fires, Fire Saf. J. 99 (2018) 27–37.
[45] Y. Li, D. Xu, H. Huang, J. Zhao, J. Shuai, An experimental study on the burning rate of a continuously released n-heptane spill fire on an open water surface, J. Loss Prev. Process. Ind. 63 (2020), 104033.
[46] M. Henry, T. Klem, Scores Die in Tank Fire Boilover, Fire Service Today, 1983, pp. 11–13.
[47] K. Hasegavva, Experimental study on the mechanism of hot zone formation in open-tank fires, Fire Saf. Sci. 2 (1989) 221–230.
[48] H. Hall, Oil tank fire boilover, Mech. Eng. 47 (1925) 540.
[49] M. Arai, K. Saito, R.A. Altenkirch, A study of boilover in liquid pool fires supported on water Part I: effects of a water sublayer on pool fires, Combust. Sci. Technol. 71 (1990) 25–40.
[50] VANTELON JPGAJP, Boilover Burning of Oil Spilled on Water, 25, Twenty-Fifth Symposium (International) on Combustion/The Combustion Institute, 1994, pp. 1481–1488.
[51] J.P. Garo, J.P. Vantelon, H. Koseki, Thin-layer boilover: prediction of its onset and intensity, Combust. Sci. Technol. 178 (2006) 1217–1235.
[52] K. Inamura Ts, K.A. Tagavi, A study of boilover in liquid pool fires supported on water. Part II: effects of in-depth radiation absorption, Combust. Sci. Technol. 86 (1992) 105–119.
[53] W.C. Fan JshaGXL, Experimental study of the premonitory phenomena of boilover in liquid pool fires supported on water, J. Loss Prev. Process. Ind. 8 (1995) 21–227.
[54] F. Ferrero, M. Munoz, B. Kozanoglu, J. Casal, J. Arnaldos, Experimental study of thin-layer boilover in large-scale pool fires, J. Hazard Mater. 137 (2006) 1293–1302.
[55] D. Kong, X. Zhao, J. Chen, H. Yang, J. Du, Study on hazard characteristics and safety distance of small-scale boilover fire, Int. J. Therm. Sci. (2021) 164.
[56] D. Kong, P. Liu, J. Zhang, M. Fan, C. Tao, Small scale experiment study on the characteristics of boilover, J. Loss Prev. Process. Ind. 48 (2017) 101–110.
[57] J.P. Garo, J.P. Vantelon, Thin layer boilover of pure or multicomponet fuels, in: V.E. Zarko, V. Weiser, N. Eisenreich, A.A. Vasil'ev (Eds.), Prevention of Hazardous Fires and Explosions. The Transfer to Civil Applications of Military Experiences,, NATO Science Series, Series 1 Disarmament Technology, 26, Kluwer Academic, Dordrecht, 1999, pp. 167–182.
[58] HKaT. Yumoto, Air entrainment and thermal radiation from heptane pool fires, Fire Technol. 24 (1988) 33–47.
[59] B.M. Cetegen, A phenomenological model of near-field fire entrainment, Fire Saf. J. 31 (1998) 299–312.
[60] B.M. Cetegen, E.E. Zukoski, T. Kubota, Entrainment in the near and far field of fire plumes, Combust. Sci. Technol. 39 (1984) 305–331.
[61] C. Tao, Y. Liu, F. Tang, Q. Wang, An experimental investigation of the flame height and air entrainment of ring pool fire, Fuel 216 (2018) 734–737.
[62] C.F. Tao, Y. Shen, R.W. Zong, F. Tang, An experimental study of flame height and air entrainment of buoyancy-controlled jet flames with sidewalls, Fuel 183 (2016) 164–169.
[63] H. Wan, L. Yu, J. Ji, Quantitative analysis of the influence of air entrainment restriction degree on burning characteristics of two parallel rectangular pool fires in still air, Fire Technol. 57 (2020) 1149–1165.
[64] J. Liu, Z. Zhou, M. Chen, Experimental investigation on the effect of ambient pressure on entrainment coefficient of pool fires, Appl. Therm. Eng. 148 (2019) 939–943.
[65] H.A. Becker Sy, Entrainment, momentum flux and temperature in vertical free turbulent diffusion flames, Combust. Flame 33 (1978) 123–149.
[66] P.H. Thomas Rb, A.J.M. Heselden, Buoyant diffusion flames: some measurements of air entrainment, heat transfer, and flame merging, Symp. (Int.) Combust. 10 (1965) 983–996.
[67] B. McCaffrey, Entrainment and Heat Flux of Buoyant Diffusion Flames, NBSIR, 1982, pp. 82–2473.
[68] E.E. Zukoski TkaBC, Entrainment in fire plumes, Fire Saf. J. 3 (1980) 107–121.
[69] Stephen James Toner, E.E. Zukoski, T. Kubota, Entrainment, Chemistry, and Structure of Fire Plumes, Diss. California Institute of Technology, 1987.
[70] B.J. McCaffrey, Purely Buoyant Diffusion Flames: Some Experimental Results, NBSIR 79-1910, National Bureau of Standards, 1979.
[71] GORE XCZaJP, Air entrainment flow field induced by a pool fire, Combust. Flame 100 (1995) 52–60.
[72] X.C. Zhou Jpg, Measurements and Prediction of Air Entrainment Rates of Pool Fires, 26, Twenty-Sixth Symposium (International) on Combustion/The Combustion Institute, 1996, pp. 453–1459.
[73] FrancescoTamanini, Direct measurements of the longitudinal variation of burning rate and product yield in turbulent diffusion flames, Combust. Flame 51 (1983) 231–243.
[74] G. Heskestad, Luminous heights of turbulent diffusion flames, Fire Saf. J. 5 (1983) 103–108.
[75] E.E. Zukoski Bmcatk, Visible structure of buoyant diffusion flames, Symp. (Int.) Combust. 20 (1985) 361–366.
[76] J.G. Quintiere, Fundamentals of Fire Phenomena, Wiley, New York, 2006.
[77] B. Trevor, J.W.B. Maynard, A physical model for flame height intermittency, Fire Technol. 54 (2018) 135–161.
[78] B. McCaffrey, Flame Height SFPE Handbook of Fire Protection Engineering, 1995.
[79] A. Hamins Kk, P. Borthwick, T. Kashiwagi, Global properties of gaseous pool fires, Symp. (Int.) Combust. 26 (1996) 1429–1436.

[80] X. Huang, T. Huang, X. Zhuo, F. Tang, L. He, J. Wen, A global model for flame pulsation frequency of buoyancy-controlled rectangular gas fuel fire with different boundaries, Fuel (2021) 289.
[81] B.M. Cetegen, K.D. Kasper, Experiments on the oscillatory behavior of buoyant plumes of helium and helium-air mixtures, Phys. Fluids 8 (1996) 2974–2984.
[82] A. Hamins Jcytk, An experimental investigation of pulsation frequency of flames, Twenty-Fourth Symp. Int. Combust. 24 (1992) 1695–1702.
[83] B.M. Cetegen Yd, Experiments on the instability modes of buoyant diffusion flames and effects of ambient atmosphere on the instabilities, Exp. Fluid 28 (2000) 546–558.
[84] B.M. Cetegen, Behavior of naturally unstable and periodically forced axisymmetric buoyant plumes of helium and helium–air mixtures, Phys. Fluids 9 (1997) 3742–3752.
[85] R. Portscht, Studies on characteristic fluctuations of the flame radiation emitted by fires, Combust. Sci. Technol. 10 (1–2) (1975) 73–84.
[86] J. Liu, Y. He, Z. Zhou, W. Yao, R. Yuen, J. Wang, The burning behaviors of pool fire flames under low pressure, Fire Mater. 40 (2016) 318–334.
[87] R.T. Jun Fang, Jin-fu Guan, Jin-jun Wang, Yong mingZhang, Influence of low air pressure on combustion characteristics and flame pulsation frequency of pool fires, Fuel 90 (2011) 2760–2766.
[88] X. Zhang, X. Fang, L. Hu, Buoyant turbulent diffusion flame heights of free-, wall- and corner air entrainment conditions: experiments and global model based on mirror approach, Fuel (2021) 303.
[89] X. Zhang, X. Fang, Y. Miao, L. Hu, Experimental study on pulsation frequency of free-, wall- and corner buoyant turbulent diffusion flames, Fuel (2020) 276.
[90] G.W. Mulholland Wl, H. Koseki, The effect of pool diameter on the properties of smoke produced by crude oil fires, Symp. (Int.) Combust. 26 (1996) 1445–1452.
[91] C.R. Shaddix, A.B. Palotas, C.M. Megaridis, M.Y. Choi, N.Y.C. Yang, Soot graphitic order in laminar diffusion flames and a large-scale JP-8 pool fire, Int. J. Heat Mass Tran. 48 (17) (2005) 3604–3614.
[92] L. Brown Jms-Atkbajra, Characterization of thermal radiation spectra in 2 m pool fires, Proc. Combust. Inst. 32 (2009) 2567–2574.
[93] A. Hamins Mkjg, T. Kashiwagi, Estimate of flame radiance via a single location measurement in liquid pool fires, Combust. Flame 86 (1991) 223–228.
[94] S. Mudan K, Thermal radiation hazards from hydrocarbon pool fires, Prog. Energy Combust. Sci. 10 (1984) 59–80.
[95] D. Burgess, M. Hertzberg, Radiation from pool flames, Heat Tran. in flames 2 (1974) 413–430.
[96] K.B. McGrattan, H.R. Baum, A. Hamins, Thermal radiation from large pool fires, Inside NIST 6546 (2000).
[97] J.R. Howell, M.P. Mengüç, K. Daun, R. Siegel, Thermal Radiation Heat Transfer, CRC press, 2020.
[98] M. Munoz, E. Planas, F. Ferrero, J. Casal, Predicting the emissive power of hydrocarbon pool fires, J. Hazard Mater. 144 (2007) 725–729.
[99] F.G. Jie Ji, Tingting Qiu, Experimental and theoretical research on flame emissivity and radiative heat flux from heptane pool fires, Proc. Combust. Inst. 38 (2021) 4877–4885.
[100] P.K. Raj, Large hydrocarbon fuel pool fires: physical characteristics and thermal emission variations with height, J. Hazard Mater. 140 (2007) 280–292.
[101] H. Koseki, Combustion properties of large liquid pool fires, Fire Technol. 25 (1989) 241–255.
[102] J. Ris, Fire radiation—a review, Symp. (Int.) Combust. 17 (1979) 1003–1016.
[103] R.O. Buckius, C.L. Tien, Infrared flame radiation, Int. J. Heat Mass Tran. 20 (2) (1977) 93–106, https://doi.org/10.1016/0017-9310(77)90001-1, 0017-9310.
[104] M. Considine, Thermal Radiation Hazard Ranges from Large Hydrocarbon Pool Fires, Report No. SRD R297, Safety & Reliability Directorate, UKAtomic Energy Authority, October, 1984. WigshawLane, Culcheth,Warrington,WA3 4NE, UK.
[105] C.L. Beyler, Fire hazard calculations for large, open hydrocarbon fires, in: The SFPE Handbook of Fire Protection Engineering, third ed., National Fire Protection Association, Quincy, MA, 2002, pp. 3–268. Section 3, Chapter 11.
[106] J. Moorhouse, Scaling criteria for pool fires derived from large-scale experiments, the assessment of major hazards, I. Chem. E. Symp Series No. 71 (1982) 165–179.
[107] P. Hamins Anthony, Jcy, Takashi Kashiwagi, A Global Model for Predicting the Burning Rates of Liquid Pool Fires, NIST Interagency/Internal Report (NISTIR) - 6381, 1999.
[108] A. Hamins Sjfa, T. Kashiwagi, M.E. Klassen, J.P. Gore, Heat feedback to the fuel surface in pool fires, CombUSI. Sci. and Tuh. 97 (1994) 37–62.
[109] F.P. Lees, Loss Prevention in the Process Industries, second ed., Butterworth-Heinemann, Oxford, 1996.
[110] C.J.H. Van Den Bosh, R.A.P.M. Weterings, Methods for the Calculation of Physical Effects (Yellow Book), third ed., Committee for the Prevention of Disasters, The Hague, 2005.
[111] F. Ruochen Yang, Eugenio Turco Neto, Riza Rusli, JieJi, Could Pool Fire Alone Cause a Domino Effect, Reliability Engineering & System Safety, 2020, p. 202.
[112] Z-j Ni, Y. Wang, Z. Yin, Relative risk model for assessing domino effect in chemical process industry, Saf. Sci. 87 (2016) 156–166.
[113] M. Spoelstra, S. Mahesh, E. Kooi, P. Heezen, Domino effects at LPG and propane storage sites in The Netherlands, Reliab. Eng. Syst. Saf. 143 (2015) 85–90.
[114] Stefania Benucci, Giovanni Uguccioni, Fire hazard calculations for hydrocarbon pool fires–application of "fire dynamics simulator–fds" to the risk assessment of an oil extraction platform, Chem. Eng. Trans. 19 (2010) 291–296.
[115] L. Zhuang Wu, Shouzhi Wu, Xingguang Wu, Fangyuan Liu, The time-to-failure assessment of large crude oil storage tank exposed to pool fire, Fire Saf. J. (2020) 117.
[116] R. Adityo, R. Agung, P. Satrio, Y.S. Nugroho, Measurement of thermal radiative heat transfer using a multi-axis heat flux sensor, in: 2nd International Tropical Renewable Energy Conference (I-TREC), IOP Conf. Series: Earth and Environmental Science, 105, 2018, 012106.
[117] Johan Sjostrom, Francine, Glenn Appel, Henry Persson, Thermal exposure from large scale ethanol fuel pool fires, Fire Saf. J. 78 (2015) 229–237.
[118] A. Di Padova, A. Tugnoli, V. Cozzani, T. Barbaresi, F. Tallone, Identification of fireproofing zones in Oil&Gas facilities by a risk-based procedure, J. Hazard Mater. 191 (2011) 83–93.
[119] J. Wu, H. Zhu, Y. Hu, Numerical simulation and risk analysis on large-scale oil tank farm conflagration based upon FDS, IOP Conf. Ser. Earth Environ. Sci. 565 (2020), 012010.
[120] M. Li, C. Zhang, C. Wang, Z. Liu, B. Wang, Ignition behavior and critical distance of flammable liquids by radiant heat flux from adjacent pool fire, Int. J. Therm. Sci. (2021) 168.
[121] H. Wan, Z. Gao, J. Ji, Y. Zhang, Experimental study on flame radiant heat flux from two heptane storage pools and its application to estimating safety distance, Energy 182 (2019) 11–20.
[122] H. Wan, Z. Gao, J. Ji, Y. Zhang, K. Li, L. Wang, Effects of pool size and spacing on burning rate and flame height of two square heptane pool fires, J. Hazard Mater. 369 (2019) 116–124.
[123] S. Vasanth Smt, Tasneem Abbasi, S.A. Abbasi, Multiple pool fires:Occurrence, simulation,modeling and management, J. Loss Prev. Process. Ind. 29 (2014) 103–121.
[124] A.S. Fanliang Ge, Jie Ji, Huaxian Wan Experimental Study on the Evolution of Heat Feedback in Multiple Pool Fires, Proceedings of the Combustion Institute, 2020.
[125] Q.L. Naian Liu, Jesse S. Lozano, Linhe Zhang, Zhihua Deng, Bin Yao, Jiping Zhu, KohyuSatoh, Multiple fire interactions: a further investigation by buring rate data of square fire arrays, Proc. Combust. Inst. 34 (2013) 2555–2564.
[126] N. Liu, Q. Liu, J.S. Lozano, L. Shu, L. Zhang, J. Zhu, Z. Deng, K. Satoh, Global burning rate of square fire arrays: experimental correlation and interpretation, Proc. Combust. Inst. 32 (2009) 2519–2526.
[127] D. Pantousa, Numerical study on thermal buckling of empty thin-walled steel tanks under multiple pool-fire scenarios, Thin-Walled Struct. 131 (2018) 577–594.
[128] A. Sengupta, A.K. Gupta, I.M. Mishra, Engineering layout of fuel tanks in a tank farm, J. Loss Prev. Process. Ind. 24 (2011) 568–574.
[129] C. Chen, G. Reniers, Economic approaches for making prevention and safety investment decisions in the process industry, in: Methods in Chemical Process Safety, 4, Elsevier, 2020, pp. 355–378.
[130] Health, Safety Executive, Risk Criteria for Land-Use Planning in the Vicinity of Major Industrial Hazards, 1989.
[131] Frank Lees, Lees' Loss Prevention in the Process Industries: Hazard Identification, Assessment and Control, Butterworth-Heinemann, 2012.
[132] Demetrio Egidi, F.P.F. Gigliola Spadoni, Aniello Amendola, The ARIPAR project: analysis of the major accident risks connected with industrial and transportation activities in the Ravenna area, Reliab. Eng. Syst. Saf. 49 (1995) 75–89.
[133] J.M. Chatris Jq, J. Folch, E. Planas, J. Arnaldos aJC, Experimental study of burning rate in hydrocarbon pool fires, Combust. Flame 126 (2001) 1373–1383.
[134] D. Burgess, M. Hertzberg, in: N.H. Afgan, J.M. Beers (Eds.), Radiation from Pool Flames, 1974.
[135] C. Kuang, L. Hu, X. Zhang, Y. Lin, L.W. Kostiuk, An experimental study on the burning rates of n-heptane pool fires with various lip heights in cross flow, Combust. Flame 201 (2019) 93–103.
[136] Z.H. Zhou, Y. Wei, H.H. Li, R. Yuen, W. Jian, Experimental analysis of low air pressure influences on fire plumes, Int. J. Heat Mass Tran. 70 (2014) 578–585.
[137] P. Zhu, Z.X. Tao, C. Li, Q.Y. Liu, Q. Shao, R. Yang, H. Zhang, Experimental study on the burning rates of Ethanol-Gasoline blends pool fires under low ambient pressure, Fuel 252 (2019) 304–315.
[138] J.P. GaroJ, P. VantelonA, C. Fernande-Pello, Effect of the fuel boiling point on the boilover burning of liquid fuels spilled on water, Symp. (Int.) Combust. 26 (1996) 1461–1467.
[139] J.H. Burgoyne, L.L. Katan, Fires in open tanks of petroleum products: some fundamental aspects, J. Inst. Petrol. 33 (1947) 158.
[140] C.L. Tien, K.Y. Lee, A.J. Stretton, Radiation heat transfer." SFPE handbook of fire protection engineering 3, 2002.
[141] A. Bouhafid Jpv, J.M. Souil, G. Bosseboeuf, F.X. Rongere, Characterisation of thermal radiation from freely burning oil pool fires, Fire Saf. J. 15 (1989) 367–390.
[142] G. Heskestad, On Q* and the dynamics of turbulent diffusion flames, Fire Saf. J. 30 (1998) 215–227.
[143] E.E. Zukoski, T. Kubota, B. Cetegen, Entrainment in the near field of a fire plume. NASA STI/Recon Technical Report N 82, 1981, 26517.
[144] M. Munoz, J. Arnaldos, J. Casal, E. Planas, Anal y sis of the geometric and radiative characteristics of hy drocarbon pool fires, Combust. Flame 139 (3) (2004) 263–277.
[145] M. Klassen Jpg, Temperature and soot volume fraction statistics in toluene-fired pool fires, Combust. Flame 93 (1993) 270–278.
[146] Christopher R. Shaddix Kcs, Laser-induced incandescence measurements of soot production, Combust. Flame 107 (1996) 418–452.
[147] H. MichaelFrenklach, Detailed modeling of soot particle nucleation and growth, Symp. (Int.) Combust. 23 (1991) 1559–1566.
[148] C. Kermit, J.H. Smyth, Robert C. Dorfman, W. GaryMallard, Robert J. Santoro, Soot inception in a methane or air diffusion flame as characterized by detailed species profiles, Combust. Flame 62 (1985) 157–181.
[149] O.S. Burgess, A. Strasser, J. Grumer, Diffusive burning of liquid fuels in open trays, Fire Res. Abstr. Rev. 3 (1961) 177.

[150] A.T. Modak, Thermal radiation from pool fires, Combust. Flame 29 (1977) 177–192.
[151] P.J. Rew Wgh, D.M. Deaves, Modelling of thermal radiation from external hydrocarbon pool fires, Process Saf. Environ. Protect. 75 (1997) 81–89.
[152] M. Munoz, J. Arnaldos, C. Planas, Analysis of the geometric and radiative characteristics of hydrocarbon pool fires, Combust. Flame 139 (2004) 263–277.
[153] M. Shokri, C.L. Beyler, Radiation from larger pool fires, SEPE J. Fire Protect. Eng. 4 (1) (1989) 141–150.